

JGR Atmospheres

RESEARCH ARTICLE

10.1029/2023JD039735

Key Points:

- The spatiotemporal characteristics of different types of droughts in each sub-region exhibited expected high spatial heterogeneity
- The drought propagation time was shorter and the relationship between droughts was closer in southeast China than in northwest China
- Climatic conditions played a dominant role in the propagation from meteorological to agricultural and hydrological droughts

Supporting Information:

Supporting Information may be found in the online version of this article.

Correspondence to:

Y. Xu,
xuyy@nju.edu.cn

Citation:

Cheng, X., Xu, Y., Chen, J., & Liu, Q. (2023). The impact of climatic conditions, human activities, and catchment characteristics on the propagation from meteorological to agricultural and hydrological droughts in China. *Journal of Geophysical Research: Atmospheres*, 128, e2023JD039735. <https://doi.org/10.1029/2023JD039735>

Received 1 AUG 2023

Accepted 6 DEC 2023

Author Contributions:

Conceptualization: Xing Cheng, Yuyue Xu

Data curation: Xing Cheng

Funding acquisition: Yuyue Xu

Methodology: Xing Cheng

Project Administration: Yuyue Xu

Resources: Xing Cheng

Supervision: Yuyue Xu

Writing – original draft: Xing Cheng, Yuyue Xu, Jianli Chen, Qing Liu

Writing – review & editing: Xing Cheng, Yuyue Xu, Jianli Chen, Qing Liu

The Impact of Climatic Conditions, Human Activities, and Catchment Characteristics on the Propagation From Meteorological to Agricultural and Hydrological Droughts in China

Xing Cheng^{1,2} , Yuyue Xu^{1,2,3} , Jianli Chen⁴ , and Qing Liu^{1,2}

¹School of Geography and Ocean Science, Nanjing University, Nanjing, China, ²Jiangsu Provincial Key Laboratory of Geographic Information Science and Technology, Nanjing University, Nanjing, China, ³Frontiers Science Center for Critical Earth Material Cycling, Nanjing University, Nanjing, China, ⁴Department of Land Surveying and Geo-Informatics and Research Institute for Land and Space, The Hong Kong Polytechnic University, Kowloon, China

Abstract Droughts are one of the most frequent and destructive natural disasters worldwide. In the past decades, drought events in China are frequent and caused severe socio-economic losses. To better predict and manage droughts, the spatiotemporal characteristics of the three types of droughts and propagation time (PT) from meteorological to agricultural and hydrological droughts in China during 1982–2014 were analyzed based on drought indices, while the causes of drought propagation were discussed. The results showed that meteorological droughts exhibited an insignificant trend. Agricultural droughts mainly aggravated in the northeastern and central regions. And the hydrological droughts were long-lasting and exacerbated in most areas. The propagation speed from meteorological to agricultural and hydrological droughts was extremely rapid (1–2 months) in southeast China, and the relationships among droughts were close (correlation coefficient/ $R > 0.6$). The propagation from meteorological to hydrological droughts was slower (6–8 months) in central China. In northwest China, the association between meteorological and hydrological droughts was weak ($R < 0.4$). Climatic conditions (especially temperature) played a dominant role in the propagation from meteorological to agricultural and hydrological droughts, explaining 63.3% and 52.6% of the variations in the PT, respectively. Urbanization, agricultural activities, elevation, and vegetation contributed to the propagation from meteorological to agricultural droughts. Reservoirs, agricultural activities, and vegetation also affected the propagation from meteorological to hydrological droughts by regulating hydrological processes. These findings are of vital significance to the prediction, warning, and management of different droughts.

Plain Language Summary With climate change and increased water demand caused by population growth, the risk of global drought events has increased dramatically. It is indispensable to understand the mechanism of drought development and monitor drought events accurately. However, there is a lack of research on the systematic and quantitative evaluation of the driving forces of drought propagation across entire China. In this study, drought propagation has been discussed from both qualitative and quantitative perspectives based on several crucial factors (climatic conditions, human activities, and catchment characteristics). Results showed that drought propagation witnessed intensive spatial heterogeneity in China. The propagation from meteorological to agricultural and hydrological droughts was exceedingly rapid (1–2 months) in southeast China, and the relationships among droughts were close. The propagation from meteorological to hydrological droughts was slower (6–8 months) in central China. In northwest China, the connection between meteorological and hydrological droughts was weak ($R < 0.4$). Climatic conditions played a dominant role in the propagation from meteorological to agricultural and hydrological droughts, explaining the variations of 63.3% and 52.6% in the propagation time, respectively. These findings are of vital significance to the prediction, warning, and management of different types of droughts.

1. Introduction

Droughts are one of the most devastating hazards worldwide (Dai, 2010; van Loon, 2013; F. Yang et al., 2021), and they refer to the period when water availability is consistently below the normal level (Van Loon & Laaha, 2015). With climate change and increased water demand caused by population growth, the risk of global drought events has increased dramatically (Dai, 2012; Mishra & Singh, 2010). Owing to the influence of the monsoon climate,

several prolonged and severe droughts have occurred in China during the past decades, which have impeded the ecology, environment, agriculture, society, and economy (Long et al., 2014, 2020; W. Wang et al., 2016; Xu et al., 2022; X. Yang et al., 2020; Yao et al., 2018). For example, severe droughts resulted in huge socio-economic losses in most areas of northern China in 1997 and 1999–2002 (Mishra & Singh, 2010). Southwest China experienced a serious drought during 2009–2010, which led to a lack of drinking water for more than nine million residents (Ayantobo et al., 2017; Lin et al., 2015). In 2010, widespread droughts in China hampered crop growth (Van Loon, 2015). The huge losses caused by drought have arrested universal attention (He et al., 2020; Spinoni et al., 2014; M. Wang et al., 2021; T. Wang et al., 2021). It is indispensable to understand the mechanism of drought development and monitor drought events accurately, which will provide an effective early warning for humans.

Droughts can be classified into four types: meteorological, agricultural, hydrological, and socioeconomic droughts (West et al., 2019; Wilhite & Glantz, 1985). The first three types fall into environmental droughts, which can reflect different kinds of water resource deficits. Meteorological drought (MD) is usually caused by accumulated precipitation deficits over several months. Agricultural drought (AD) occurs when soil moisture decreases to the point where it affects crop and vegetation growth (Martínez-Fernández et al., 2016; Shen et al., 2019). Hydrological drought is the period during which surface water or groundwater is consistently below normal values (Vicente-Serrano et al., 2012). Socioeconomic drought is regarded as a water resource system drought (Loukas & Vasiliades, 2004), which refers to the situation in which the supply of water cannot meet demand. Socioeconomic drought reflects the impact on socioeconomic and human activities (S. Liu et al., 2020; Tu et al., 2018). There are close interactions between the different types of droughts (Van Loon, 2015; West et al., 2019). In general, meteorological droughts occur first in a region when precipitation decreases continuously over a period. The causes of the extreme decrease in precipitation varied in different regions and seasons, such as global warming and the change in atmospheric circulation impacted by El Niño and Southern Oscillation (Larkin & Harrison, 2005; Mason & Goddard, 2001; R. Zhang et al., 1999). Then, with strong evapotranspiration caused by high temperatures and continuous precipitation deficits, soil moisture might decrease simultaneously, and surface runoff and groundwater flow will reduce to a low level through the hydrological cycle. In these cases, agricultural and hydrological droughts will develop in this region, which is defined as drought propagation (Leng et al., 2015; A. Zhang & Jia, 2013). Revealing the propagation time (PT) and relationships among meteorological, agricultural, and hydrological droughts will provide early warning and management for agricultural and hydrological droughts when precipitation anomalies and extremely high temperatures occur in a region, and then the damages caused by compound droughts will be attenuated.

In recent years, global drought events are frequent and researchers have conducted several national-scale studies on drought propagation, such as those in the United States (Apurv & Cai, 2020; Tjeldeman et al., 2018), German (Stahl & Heudorfer, 2017), the United Kingdom (Barker et al., 2016), South Korea (Bae et al., 2019), India (Bhardwaj et al., 2020; Das et al., 2022), Brazil (Bevacqua et al., 2021), and Thailand (Zhao et al., 2022). Due to the influence of the monsoon climate, China is also a country prone to drought (Long et al., 2020; Xu et al., 2022; X. Yang et al., 2020). Many scholars have also discussed the mechanisms and driving forces of drought propagation in China on a regional scale, including the Loess Plateau (J. Wu et al., 2018), the Luan River Basin (Xu et al., 2019), the Pearl River Basin (Z. Zhou et al., 2021b), the Yangtze and Yellow River basins (Li et al., 2020; H. Zhang et al., 2021), and the Longchuan River Basin (F. Yang et al., 2021). In addition, several studies on drought propagation have also been performed across entire China. For example, Xu et al. (2021) found that the propagation speed from meteorological to agricultural droughts in China depended on the climate type. The PT was shorter in humid areas than in other regions because of the fast response to precipitation anomalies caused by the rapid water cycle in humid regions. Ding, Gong, et al. (2021) found that the drought propagation relationship between meteorological droughts and agricultural droughts varied in different seasons. The connection between droughts was stronger in growing season and summer than in spring and autumn, because more precipitation can be applied to supply soil moisture and runoff in summer. In addition to climate and season, Ding, Xu, et al. (2021) also found that land cover and topography might affect the PT from meteorological to hydrological drought in China. For instance, different kinds of vegetation (such as forest, grassland, and cropland) regulate water resources and the water cycle in various ways, thus influencing the relationship between precipitation, runoff, and soil moisture differently. F. Wang et al. (2022) revealed that the propagation from meteorological to agricultural droughts was slower in winter than in summer because high temperatures and strong evapotranspiration will accelerate the propagation in summer. Anthropogenic activities might also affect the process of

drought propagation by changing land-atmosphere energy and water exchange. Q. Zhang et al. (2022) showed that the river-flow routing effect can alter the sensitivity of HD to MD, and propagation from meteorological to HD was shorter in China with higher precipitation and runoff. However, most of the current studies have mainly focused on the seasonality and regionality of drought propagation, and discussed the causes of drought propagation briefly and qualitatively based on only a part of factors.

In fact, drought propagation is subject to a wide range of complicated factors, such as human activities, for example, urbanization (T. Zhang et al., 2022), the construction of dams and reservoirs (Huang et al., 2021), agricultural irrigation and production (Ding, Xu, et al., 2021), land use and land cover (J. Wu et al., 2022), catchment characteristics, for example, terrain (J. Wu et al., 2015), vegetation cover (Huang et al., 2015), elevation (van Loon, 2013), and climatic conditions, for example, temperature (Van Loon et al., 2012), aridity and humidity (K. Zhou et al., 2021), evapotranspiration (Fang et al., 2020). Knowledge of these influencing factors is of great importance in monitoring and warning of drought from a drought propagation perspective. There is a lack of research on the systematic and quantitative evaluation of the driving forces of drought propagation across entire China. So, in this study, drought propagation has been discussed from both qualitative and quantitative perspectives based on several crucial factors (climatic conditions, human activities, and catchment characteristics) and the relative contribution (RC) to drought propagation has been compared, which will contribute to the further comprehension of the propagation process of droughts in China.

Based on the standardized drought indices, we have explored the characteristics (spatiotemporal trends, number of drought events, duration, intensity, and severity) of meteorological, agricultural, and hydrological droughts in China from 1982 to 2014. Then, the PT from meteorological to agricultural and hydrological droughts was calculated. The causes of drought propagation were discussed based on human activities, catchment characteristics, and climatic conditions. Our study provides a systematic understanding of the drought conditions and propagation in China over the past three decades. These findings are meaningful for the prediction, warning, and management of hydrological and agricultural droughts, which can be regarded as input and prerequisites for the construction of prediction models.

2. Study Area and Data Sets

2.1. Study Area

China has a land area of about 9.6 million km² and is located in east Asia (J. Wu et al., 2015). China's topography is complex and diverse, and the elevation in China is high in the west and low in the east, analogous to the three-step ladder distribution (Y. Wang et al., 2017; Z. Wang et al., 2017). The spatial distributions of temperature and precipitation are uneven, and both are higher in southern and eastern China (Figure 1). In 2010, the average air temperature and the average annual precipitation in China were 7.9°C and 717.5 mm, respectively. According to the characteristics of climate, terrain, agriculture, and water resources, China was divided into nine typical sub-regions (Figure 1 and Table 1), including the Northeast China Plain (I), the Huang-Huai-Hai Plain (II), the Loess Plateau (III), the Northern arid and semiarid region (IV), the Qinghai Tibet Plateau (V), the Sichuan Basin and surrounding regions (VI), the Middle–Lower Yangtze Plain (VII), the Southern China region (VIII), and the Yunnan-Guizhou Plateau (IX). The division fashion was one of the most widely used modes in China, which was obtained from the Resource and Environment Science and Data Center (RESDC, <https://www.resdc.cn/>). Each region consists of several sub-regions, including provinces, municipalities, and autonomous regions. There are a total of 32 sub-regions, as shown in Figure S1 of Supporting Information S1.

2.2. Data Sets

The precipitation data used to calculate the SPI were obtained from the Full Data Monthly Product V. 2020 from the Global Precipitation Climatology Centre (GPCC) with a spatial resolution of 0.5° (<https://opendata.dwd.de/>, Table 2). The GPCC was established in 1989 to collect, assess, and analyze global precipitation station data (Becker et al., 2013). Among all the GPCC products, the full-data product is the most common and accurate reanalysis data set (Sun et al., 2018), and this data set has been used in many studies on hydrology and climatology. We used the soil moisture data of the 0–10 cm soil layers from the Global Land Data Assimilation System (GLDAS) version 2.0, Noah Land Surface Model (LSM) L4 monthly data set with a spatial resolution of 0.25° to represent the land surface soil moisture condition and calculate the SSMI, which was jointly developed

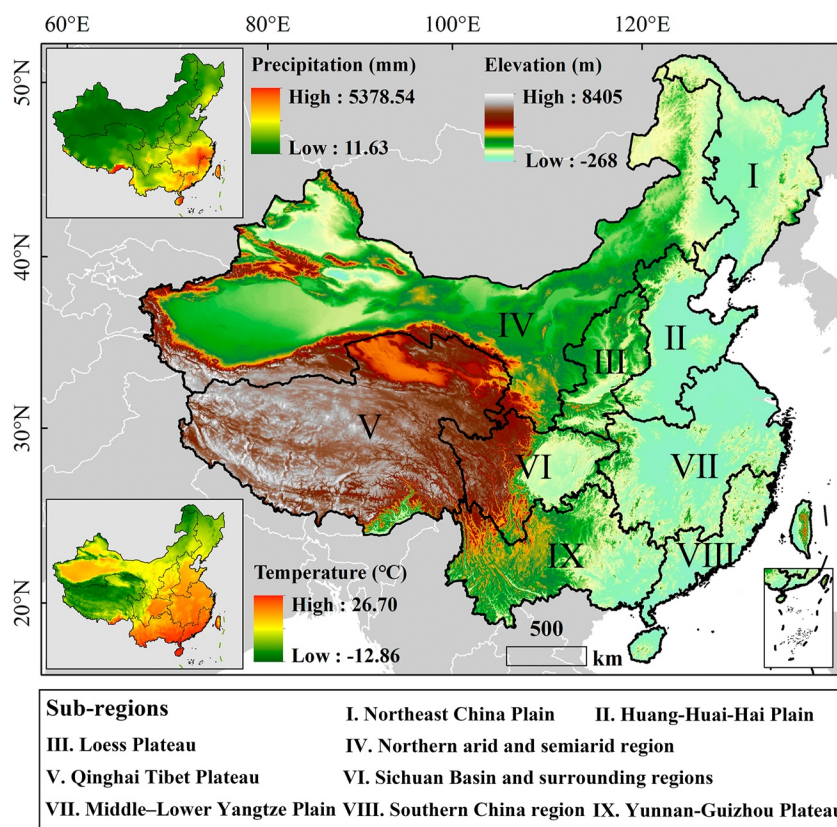


Figure 1. The geographical location of China and the spatial distribution of sub-regions, average air temperature (left bottom), and average precipitation (left top) in China in 2010. There are nine sub-regions, including the Northeast China Plain (I), the Huang-Huai-Hai Plain (II), the Loess Plateau (III), the Northern arid and semiarid region (IV), the Qinghai Tibet Plateau (V), the Sichuan Basin and surrounding regions (VI), the Middle-Lower Yangtze Plain (VII), the Southern China region (VIII), and the Yunnan-Guizhou Plateau (IX).

by the National Aeronautics and Space Administration (NASA) and the National Oceanic and Atmospheric Administration (NOAA) (<https://disc.gsfc.nasa.gov/>). This data set was obtained by averaging the reprocessed 3-hourly data, including many land surface parameters simulated by Noah Model 3.6. It has been one of the root zone soil moisture products for more than 30 years (X. Zhang et al., 2017). Runoff data from the 0.5° Global

Table 1
Average Elevation, Average Precipitation, Average Air Temperature, Total Runoff, and Administrative Divisions in 2010 in Nine Sub-Regions in China

Region ID	Average elevation (m)	Average precipitation (mm)	Average air temperature (°C)	Total runoff (mm)	Administrative division
I	323.73	679.34	2.55	96.34	Heilongjiang, Jilin, and Liaoning Provinces (3)
II	311.50	664.55	12.35	51.21	Hebei, Henan, Shandong Provinces and Beijing, Tianjin Cities (5)
III	1142.84	584.20	10.40	64.40	Shanxi and Shanxi Provinces (2)
IV	1589.42	217.755	5.23	51.52	Xinjiang, Inner Mongolia, Ningxia, and Gansu Provinces (4)
V	4467.11	471.81	-0.93	352.34	Qinghai and Xizang Provinces (2)
VI	2317.42	918.04	10.26	275.40	Sichuan Province and Chongqing City (2)
VII	269.67	1545.68	16.53	497.00	Jiangsu, Zhejiang, Anhui, Hunan, Hubei, Jiangxi Provinces, and Shanghai City (7)
VIII	361.16	1946.62	20.55	675.38	Guangdong, Taiwan, Fujian, Hainan Provinces and Hong Kong, Macao (6)
IX	1274.38	1233.56	17.34	296.55	Yunnan, Guizhou, and Guangxi Provinces (3)

Table 2
Summary of Data Sets Used in This Study

Items	Data sets	Spatial resolution	Temporal resolution	Time span	Source
Precipitation	GPCC V. 2020	0.5°	1 month	1982–2014	https://opendata.dwd.de/
Soil Moisture	GLDAS Noah LSM L4	0.25°	1 month	1982–2014	https://disc.gsfc.nasa.gov/
Runoff	GRUN	0.5°	1 month	1982–2014	https://figshare.com/articles/dataset/GRUN_Global_Runoff_Reconstruction/9228176
Nightlight	DMSP-OLS	0.0083°	1 year	1992–2013	https://www.resdc.cn/
Reservoir	GRanD v1.1	/	/	2011	http://globaldamwatch.org/grand/
Land Cover	ESA CCI	300 m	1 year	1992–2014	https://www.esa-landcover-cci.org/
Elevation	SRTM DEM	90 m	/	2002	https://code.earthengine.google.com/
Slope	SRTM DEM	90 m	/	2002	https://code.earthengine.google.com/
NDVI	GIMM	0.0083°	1 month	1982–2014	https://www.nasa.gov/nex
Temperature	GLDAS Noah LSM L4	0.25°	1 month	1982–2014	https://disc.gsfc.nasa.gov/
Potential evapotranspiration	GLDAS Noah LSM L4	0.25°	1 month	1982–2014	https://disc.gsfc.nasa.gov/
Actual evapotranspiration	GLDAS Noah LSM L4	0.25°	1 month	1982–2014	https://disc.gsfc.nasa.gov/

Runoff Reconstruction data set (GRUN) were used to calculate the SRI (https://figshare.com/articles/dataset/GRUN_Global_Runoff_Reconstruction/9228176). GRUN is a global runoff data set, which was calculated using the machine learning method based on in-situ streamflow observations. The predicted results agree with previous observations (Ding, Xu, et al., 2021; Ghiggi et al., 2019).

In this study, we discussed the causes of drought propagation from three aspects: human activities, catchment characteristics, and climatic conditions. First, three indicators (Nightlight, reservoir, and cropland) were used to represent human activity. (a) Nightlight information (Defense Meteorological Satellite Program-Operational Linescan System (DMSP-OLS) Nighttime Lights Time Series) was provided by the National Geophysical Data Center at NOAA (J. Wu et al., 2013; Q. Zhang & Seto, 2011), which was collected from the RESDC (<https://www.resdc.cn/>). Nighttime light is often used to indicate urban sprawl and economic development at regional and global scales (M. Wang et al., 2021; T. Wang et al., 2021). (b) Reservoir data were obtained from the Global Reservoir and Dam Database (GRanD) v1.1, which was published in 2011 and included global dam and reservoir information (<http://globaldamwatch.org/grand/>). (c) The percentages of cropland were calculated based on 300 m land cover data produced by the European Space Agency (ESA) Climate Change Initiative (CCI) (<https://www.esa-landcover-cci.org/>). All classes related to croplands were considered to obtain information about agricultural activities (Zhu et al., 2021).

Second, the catchment characteristics refer to the natural basic features in a region, so the elevation, slope, and vegetation cover were selected according to their close relationships with regional water resources and the water cycle. (a) Elevation information was captured from the Shuttle Radar Topography Mission Digital Elevation Model V4.1 data set (90 m) provided by the Google Earth Engine platform (GEE, <https://code.earthengine.google.com/>). (b) The slope was calculated based on the elevation information on the GEE platform. (c) The normalized difference vegetation index (NDVI) data of the Global Inventory Monitoring and Modeling System (GIMM) were used to reflect the vegetation cover conditions, which were provided by NASA (<https://www.nasa.gov/nex>) and collected from the National Tibetan Plateau Third Pole Environment (TPDC, <https://data.tpdc.ac.cn/en/data/>).

Third, temperature, aridity, and actual evapotranspiration were selected to indicate the climatic conditions. (a) Temperature data were from the 0.25° GLDAS version 2.0, Noah LSM L4 monthly data set. (b) The aridity index refers to the ratio of precipitation to potential evapotranspiration and is used to reflect the dryness of a region

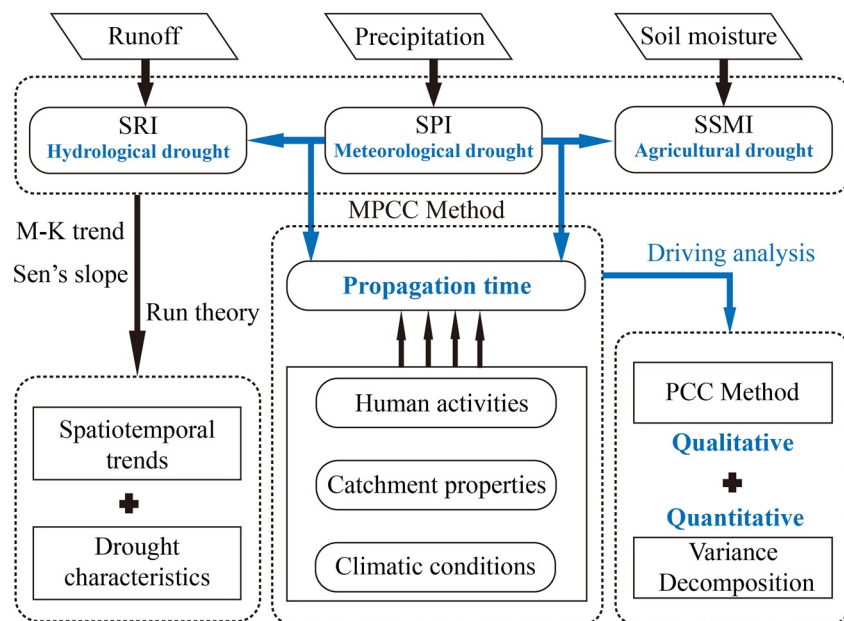


Figure 2. The flow chart of this study. The blue lines indicate the calculation process of drought propagation time and its causes. The black lines indicate the analysis of spatiotemporal trends and drought characteristics of three different types of drought. The SPI, SSMI, and SRI represent the standardized precipitation index, the standardized soil moisture index, and the standardized runoff index, respectively. M-K, Pearson correlation coefficient (PCC), and maximum Pearson correlation coefficient (MPCC) are the Mann-Kendall trend, the PCC, and the MPCC method, respectively.

(Greve et al., 2019; Nastos et al., 2013). Where a larger aridity index indicates higher humidity. Precipitation data from the GPCC product have been previously introduced. Potential evapotranspiration data were obtained from the 0.25° GLDAS version 2.0, Noah LSM L4 monthly data set. (c) The actual evapotranspiration data were also from the 0.25° GLDAS version 2.0, Noah LSM L4 monthly data set provided by NASA and NOAA (<https://disc.gsfc.nasa.gov/>).

3. Methodology

In this study, the SPI, SSMI, and SRI were applied to characterize meteorological, agricultural, and hydrological droughts in China from 1982 to 2014 (Figure 2). Then, spatiotemporal characteristics (trends, number of drought events, duration, intensity, and severity) of the three types of droughts were calculated based on the Mann-Kendall (M-K) trend analysis method, Sen's slope estimator, and run theory (Kendall, 1948; Mann, 1945; Sen, 1968; Yevjevich, 1967). Finally, we applied the maximum Pearson correlation coefficient (MPCC) method to calculate the PT from meteorological to agricultural and hydrological droughts and discussed the causes impacting drought propagation from both qualitative (the Pearson correlation coefficient (PCC) method) and quantitative (the variance decomposition method) perspectives.

3.1. Drought Indices

The drought index is one of the most widely used and effective methods for quantitative drought assessments (Zhong et al., 2019). Several drought indices have been proposed in many studies. For example, the Palmer drought severity index (PDSI, Palmer, 1965), SPI (McKee et al., 1993), SRI, (Shukla & Wood, 2008), standardized streamflow index (SSI, Vicente-Serrano et al., 2012), crop moisture index (CMI, Palmer, 1968), SSMI, (Samaniego et al., 2013), and the improved multivariate standardized reliability and resilience index (IMSRI, Guo et al., 2019a). There are advantages and disadvantages to assessing drought events using diverse drought indices (Mishra & Singh, 2010).

Standardized drought indices (including SPI, SSMI, and SRI) are simple to understand and calculate because of the low demand for data, and can describe drought conditions at different time scales (M. Wang et al., 2021; T. Wang et al., 2021; Z. Zhou et al., 2021a). Moreover, they are robust and used worldwide. For example, the SPI

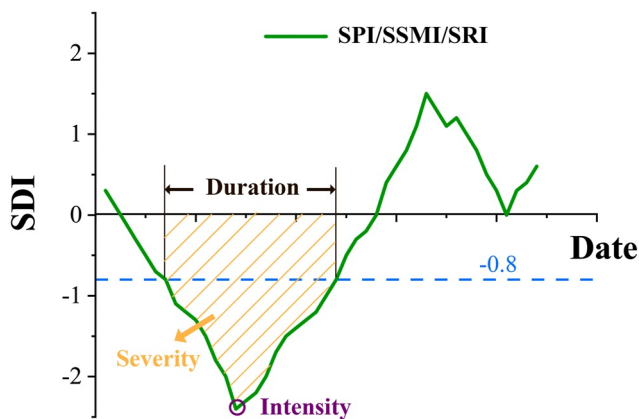


Figure 3. Introduction to drought characteristics. The green line represents the SPI, SSMI, or SRI series. The blue dotted line represents the threshold (-0.8), which is used to extract drought events. Duration is the accumulated time that the drought index is consistently below the threshold. Intensity is the minimum value of the drought index during the drought period. Severity is the sum of the drought index during the drought period.

is used by the World Meteorological Organization to monitor meteorological droughts (Xu et al., 2019), which can describe the accumulated precipitation deficiency at different time scales based on long-term precipitation series (more than 30 years, Han et al., 2019). The definition and calculation of SSMI and SRI are similar to that of SPI. Therefore, the SPI, SSMI, and SRI were chosen to track meteorological, agricultural, and HD events in China during 1982–2014.

The calculation procedure of the SPI proposed by McKee et al. (1993) is as follows. First, we calculated the n -month accumulated precipitation series ($n = 1, 2, 3, \dots, 12$) based on the original long-term precipitation series, where $n = 1, 3,$ and 12 represent the monthly, seasonal, and annual precipitation series, respectively. Then, we fitted the n -month accumulated precipitation series to calculate the cumulative probability of precipitation by applying different distribution functions (e.g., the log-normal function (Z. Zhou et al., 2021b) and gamma function (Wilks & Eggleston, 1992)). The gamma function was chosen in this study and the parameter is obtained based on the maximum likelihood estimator in MATLAB. Finally, the fitted cumulative probability was converted to a value under the standard normal distribution, which is called the SPI value. The specific formula was presented by Hao et al. (2017). The calculations of the SSMI and SRI are comparable to those of the SPI. Based on the long-term soil moisture (runoff) series, the accumulated soil moisture (runoff) deficit was captured to assess agricultural (hydrological) drought.

3.2. Spatiotemporal Characteristics of Droughts

In this study, the spatiotemporal characteristics of droughts (including trends, number of drought events, duration, intensity, and severity) in each sub-region were explored. On the one hand, the M-K trend analysis method and Sen's slope estimator were used to assess the temporal and spatial trends of droughts. The M-K trend analysis method is non-parametric, robust, widely used, and suitable for nonlinear trend assessment (Douglas et al., 2000; Shi et al., 2018; Tabari et al., 2011), and this method was proposed and improved by Mann (1945) and Kendall (1948). The result Z of the M-K method is used to reveal the significance, where $|Z| \geq 2.58$ and $|Z| \geq 1.96$ indicate the trends satisfy the significance levels of $p < 0.01$ and $p < 0.05$, respectively (J. Wu et al., 2018). Positive and negative values indicate upward and downward trends, respectively. Sen's slope estimator is a non-parametric test proposed by Sen (1968), that is applied to convert Z to a quantitative slope value. The formulas for the M-K method and Sen's slope estimator are shown in Gocic and Trajkovic (2013).

On the other hand, drought events were captured based on run theory (Yevjevich, 1967). In this study, a drought event occurred when the drought index remained below -0.8 for more than 3 months (J. Wu et al., 2018). For each drought event, three drought characteristics (duration, intensity, and severity), which are important for revealing drought conditions, were calculated (Guo et al., 2019b). The duration refers to the time at which the drought index is consistently below the threshold. The intensity and severity are defined as the minimum value and sum of the drought indices during the drought period, respectively. A detailed introduction is presented in Figure 3. In addition, the total number of drought events in China from 1982 to 2014 was counted.

3.3. Drought Propagation Time

According to the theoretical definition, drought PT is the interval between the onset of one type of drought and the onset of another (Xu et al., 2021). In this study, the MPCC method was applied to approximately calculate the PT, which is currently widely used in studies on drought propagation (Ding, Gong, et al., 2021; Ding, Xu, et al., 2021; J. Wu et al., 2018). We only considered the propagation from meteorological to agricultural and hydrological droughts, which refers to the propagation from the accumulation of precipitation deficits to soil moisture and runoff deficits (Bhardwaj et al., 2020). When the PCC between SPI- m ($m = 1, 2, 3, \dots, 12$) and SSMI-1 (or SRI-1) reaches the maximum value, the linkage between SPI- m and SSMI-1 (or SRI-1) is the

tightest, which shows m -month accumulated precipitation deficiency during the previous m months is most likely to cause the deficit of soil moisture (runoff). Therefore, the accumulated precipitation months (m) are regarded as the drought PT from meteorological to agricultural drought (HD) as an approximation. And the obtained drought PT based on the MPCC method can reflect the spatial distribution of propagation speed during the period. The calculation of the PCC was proposed by Pearson (1895), as shown in Equation 1.

$$PCC/R = \frac{\sum_{i=1}^l (x_i - \bar{x})(y_i - \bar{y})}{\sqrt{\sum_{i=1}^l (x_i - \bar{x})^2} \sqrt{\sum_{i=1}^l (y_i - \bar{y})^2}} \quad i = 1, 2, 3, \dots, l \quad (1)$$

where x and y denote SPI- m ($m = 1, 2, 3, \dots, 12$) and SSMI-1 (SRI-1), and l denotes the total months (from 1982 to 2014). The values of R are from -1 to 1 , and a larger absolute value of R indicates a closer correlation between x and y . Positive and negative values indicate a positive and negative correlation, respectively. Due to the different spatial resolutions of SPI (0.5°), SSMI (0.25°), and SRI (0.5°), SPI and SRI were resampled to 0.25° before calculating PT.

3.4. The Causes Affecting Drought Propagation

To explore the causes affecting the propagation from meteorological to agricultural and hydrological droughts, we evaluated the contributions of human activities, catchment characteristics, and climatic conditions from both qualitative and quantitative perspectives. To begin with, various factors need to be harmonized because the types and spatiotemporal resolutions of data sets chosen in this study (Table 2) differ considerably. Therefore, we pre-processed the data before calculating the correlation coefficients and contributions. Considering that the wide coverage of nine regions in China might lead to huge uncertainty and inaccuracy, to enhance the reliability of the results, we decided to calculate the contributions at a small provincial scale (32 sub-regions shown in Figure S1 of Supporting Information S1). This subdivision allowed us to obtain more data, facilitating a more robust analysis. Therefore, each province's average PT from meteorological to agricultural and hydrological droughts was calculated. Then, the number of reservoirs in each province was counted to represent the influence of reservoirs, and the multi-year average proportion of land area associated with irrigated cropland in each province was calculated to reveal agricultural activities. As for the other factors, the multi-year provincial averages were calculated. The statistical data was shown in Table S1 of Supporting Information S1. Next, the driving analysis of drought propagation was conducted based on the provincial scale.

On the one hand, the PCC/R was calculated to reveal the relationship between the PT and various factors, which could preliminarily indicate the influence of each factor on drought propagation. The formula for the PCC is given in Equation 1, where x represents the PT/the MPCC between different kinds of drought, and y represents various indicators, as shown in Table S1 of Supporting Information S1.

On the other hand, we applied the variance decomposition method to calculate the relative contributions of different factors to drought propagation. The principle of the variance decomposition method is to assess the influence of the variance of each independent variable on the variance of a dependent variable in a system, as shown by J. Wu et al. (2018). First, the variance (V) of the dependent variable y is calculated as follows.

$$V(\text{total}) = V(y) = V\left[\left(y - \sum_{i=1}^9 x_i\right) + \sum_{i=1}^9 x_i\right] \quad (2)$$

where y is the PT from meteorological to agricultural and hydrological droughts, and x_i ($i = 1, 2, 3, \dots, 9$) represents the nine influencing factors chosen in this study.

Here, $t = y - \sum_{i=1}^9 x_i$ is regarded as the distraction, which is related to the various factors. The variations $V(x_i^{\text{total}})$ related to each indicator x_i are shown in Equation 3.

$$V(x_i^{\text{total}}) = V(x_i) + \text{cov}(t, x_i) + \text{cov}(x_i, x_j) \quad i \neq j \text{ and } j = 1, 2, 3, \dots, 9 \quad (3)$$

where $\text{cov}(t, x_i)$ represents the covariance between t and x_i . The contribution (C) of each factor x_i and the relative contribution (RC) of each factor are shown as follows, which were calculated based on the variance of independent $V(x_i^{\text{total}})$ and the dependent variable $V(\text{total})$.

$$C_{x_i} = \frac{V(x_i^{\text{total}})}{V(\text{total})} \quad (4)$$

$$RC_{x_i} = \frac{(C_{x_i})^2}{\sum_{i=1}^9 (C_{x_i})^2} \quad (5)$$

The methods used in this study to calculate drought PT and analyze the causes are data-based methods. In contrast to hydrological modeling methods, these methods do not simulate the actual processes of the hydrological cycle (Apuv & Cai, 2020; Li et al., 2020), which may not reveal the true drought propagation process. However, we can obtain quantitative results based on the data and thus assess the causes and processes affecting drought propagation more accurately based on the results obtained and the available literature.

4. Results

4.1. The Spatiotemporal Characteristics of Different Droughts

The temporal series of different months accumulated SPI, SSMI, and SRI were displayed in Figures S2–S4 of Supporting Information S1. The trends of different types of droughts based on 1-, 6-, and 12-month accumulated standardized indices were also shown in Figure S5 of Supporting Information S1, which exhibited similar trends to SPI-3, SSMI-3, and SRI-3. Therefore, the three-month accumulated SPI-3, SSMI-3, and SRI-3 were selected as examples to indicate the trends of seasonal meteorological, agricultural, and hydrological droughts.

The overall magnitude and significance of the changes in SPI-3 were feeble (Figures 4a and 4b). Only 35.3% of the SPI-3 trends were significant ($p < 0.05$) in China. SPI-3 showed an obvious upward trend ($p < 0.05$) in western China where the total precipitation is low (Figure S6 in Supporting Information S1), such as 50.3% for the region V and 38.0% for the region IV, indicating that these areas had been meteorologically wetter in the past three decades. A significant downward trend in SPI-3 ($p < 0.05$) revealed that meteorological droughts aggravated in 40.6% of the western region IX.

Approximately 55.8% of the SSMI-3 in China changed considerably ($p < 0.05$), but the spatial distribution differed (Figures 4c and 4d). Areas with intensified AD were mainly located in northeastern and central China with high soil moisture (Figure S6 in Supporting Information S1), such as 73.9% for the region I, 81.9% for the region VII, 70.6% for the region IX, 50.7% for the region III, and 41.6% for the region VI ($p < 0.05$). The SSMI-3 showed a significant upward trend ($p < 0.05$) in western China with low soil moisture, especially in the northern region V and the region IV, indicating that the incidence of AD events decreased during 1982–2014.

The tendency of SRI-3 was exceedingly remarkable (Figures 4e and 4f), and approximately 66.8% of SRI-3 in China exhibited a significant trend ($p < 0.05$). In the northwest region V, the eastern region II, and the region VIII, the SRI-3 increased dramatically ($p < 0.05$), which demonstrated that the HD conditions were alleviated during 1982–2014. However, the trend of SRI-3 in most of the other regions showed a downward trend, especially in 80.6% for the region IV, 52.7% for the western region IX, and 46.9% for the region I ($p < 0.05$). The decreasing trends of SRI-3 indicated that most areas of China had experienced a hydrologically drying process in the past 30 years.

The meteorological, agricultural, and HD characteristics in all sub-regions of China were also calculated based on the 3-month accumulated SPI-3, SSMI-3, and SRI-3 values. The results showed significant differences in the characteristics (number of events, duration, intensity, and severity) of different types of droughts, which were discussed in Figure S7 of Supporting Information S1.

4.2. The Spatial Patterns of the Drought Propagation Time and Relationships

The PT from meteorological to agricultural and hydrological droughts exhibited high spatial heterogeneity, which was shorter in the southeast than in the northwest (Figures 5a and 5c). In southeast China, the propagation from meteorological to agricultural and hydrological droughts was expeditious, while the propagation from meteorological to hydrological droughts was dramatically slower in central and northwestern China. The correlation coefficients between different types of droughts varied significantly, showing downward trends from the southeast

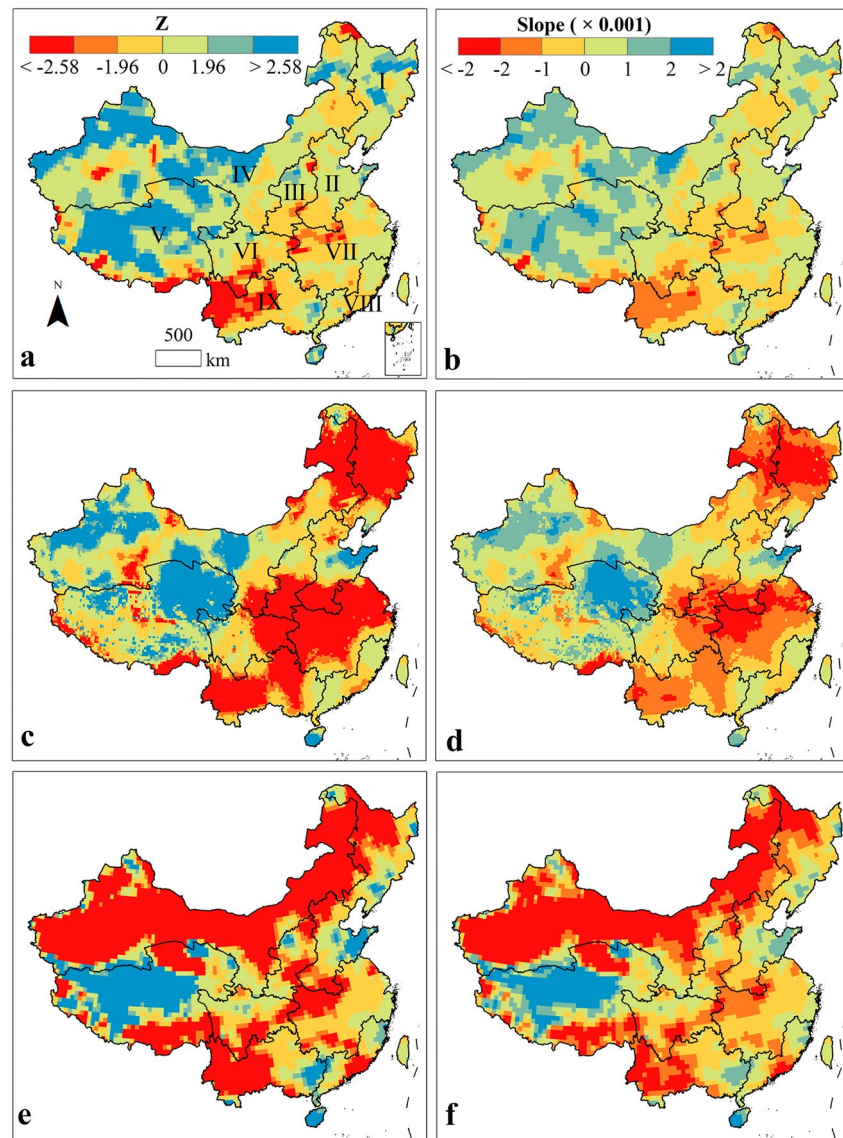


Figure 4. The spatial distribution of the Mann-Kendall trends (left) and slopes (right) for different drought indices in China from 1982 to 2014. Z represents the result of the Mann-Kendall trend analysis here, which is also used to reveal the significance. $|Z| \geq 2.58$ and $|Z| \geq 1.96$ show that the trends satisfy the significance levels of $p < 0.01$ and $p < 0.05$, respectively. These maps are the Z (a) and slope (b) of the SPI-3, the Z (c) and slope (d) of the SSMI-3, and the Z (e) and slope (f) of the SRI-3.

to northwest (Figures 5b and 5d). In southeast China, meteorological droughts were more closely associated with hydrological droughts than with agricultural droughts. Conversely, the linkage between meteorological and hydrological droughts has attenuated exceedingly in northwest China. In addition, we also revealed the differences between the PT from MD to AD and HD in Figure S8 of Supporting Information S1.

The propagation from meteorological to agricultural droughts was rapid, and the relationship between meteorological and agricultural droughts was close in most areas of China (Figures 5a and 5b). 72.6% of the PT in China ranged from 1 to 4 months, such as in the region II (98.0%), region III (99.8%), and region VI (94.9%). The propagation in 84.8% of the region VII, 99.8% of the region VIII, and 94.7% of the region IX was extremely rapid (1–2 months), and meteorological droughts were tightly associated with agricultural droughts ($R > 0.6$). In these regions, the precipitation deficit is highly susceptible to a decrease in soil moisture. The PT in 18.3% of China increased to 5–6 months, which was mainly concentrated in northeast China. And the correlation coefficients were principally between 0.4 and 0.8 in these areas. In the region V and region IV, the propagation from meteorological to

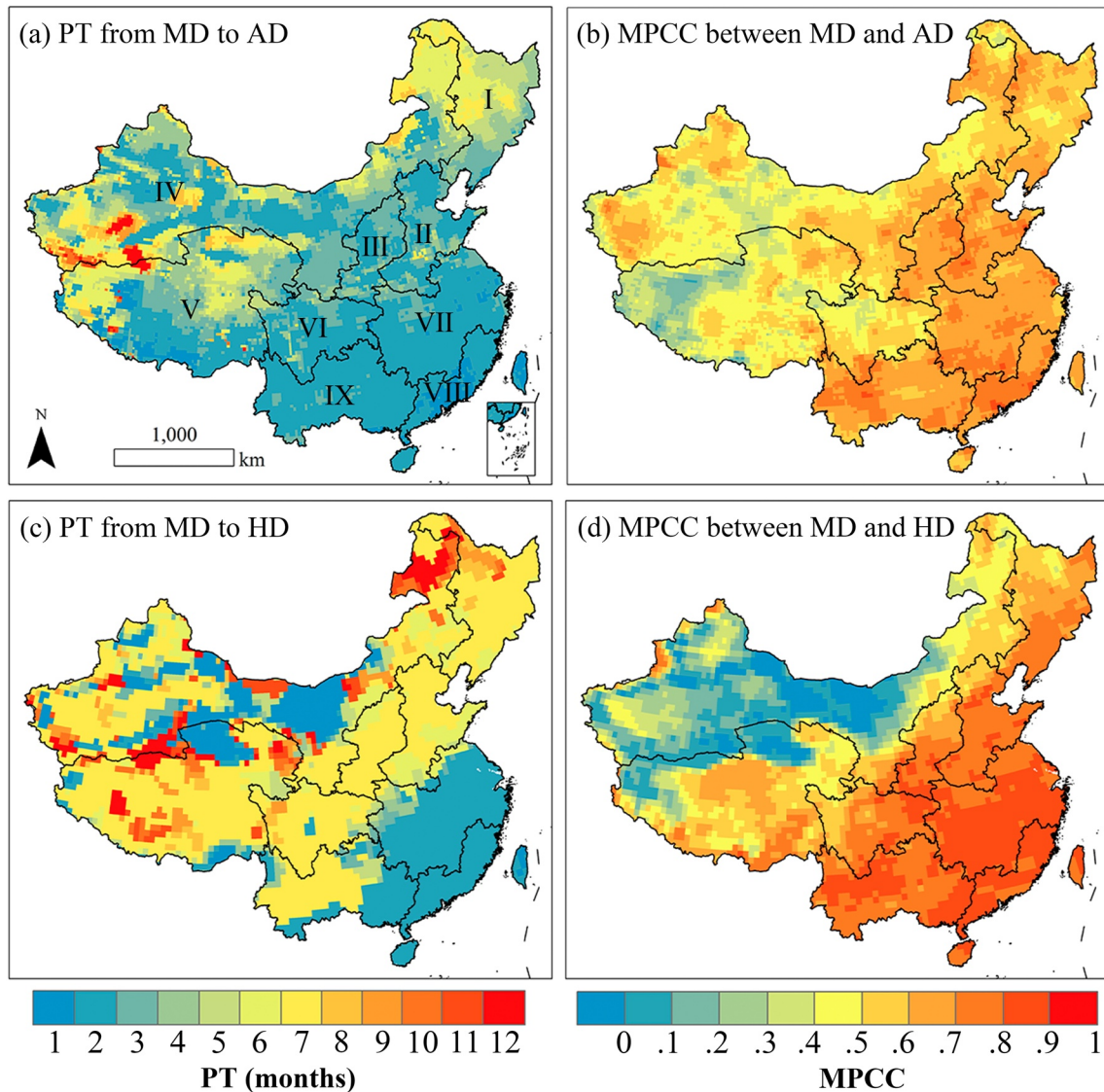


Figure 5. Spatial distribution of the propagation time (PT) and maximum Pearson correlation coefficient (MPCC) between different kinds of droughts in China, including meteorological drought (MD), agricultural drought (AD), and hydrological drought (HD). (a) These maps refer to the PT from MD to AD, (b) the MPCC between MD and AD, (c) the PT from MD to HD, and (d) the MPCC between MD and HD.

agricultural droughts was also relatively complicated. But there was a PT of 1–6 months and correlation coefficients of more than 0.4 in most regions, indicating a close relationship between meteorological and agricultural droughts.

The propagation from meteorological to hydrological droughts was geographically heterogeneous (Figures 5c and 5d). Approximately 24.5% of China showed an extremely rapid propagation (1–2 months), which was chiefly situated in the southeast, such as 80.3% of the region VII, 99.9% of the region VIII, and the eastern region IX (close to 39%). The linkage between meteorological and hydrological droughts was robust ($R > 0.8$), demonstrating that meteorological droughts were very likely to trigger hydrological droughts in these areas by transforming precipitation deficiency into streamflow scarcity. There was a longer PT of 7–8 months for 47.9% of China, where the connection between meteorological and hydrological droughts was relatively tight ($R > 0.6$). This part of the region is covered widely, mainly consisting of the region I (81.1%), region II (62.7%), region III (83.4%), and region VI (79.9%). Due to the diverse terrain and wide coverage, the mechanism underlying the propagation from meteorological to hydrological droughts was elaborate in the region V and the region IV. The correlation coefficients between meteorological and hydrological droughts were low or negative, indicating that meteorological droughts could not directly lead to hydrological droughts (Chen et al., 2020; Ding, Xu, et al., 2021).

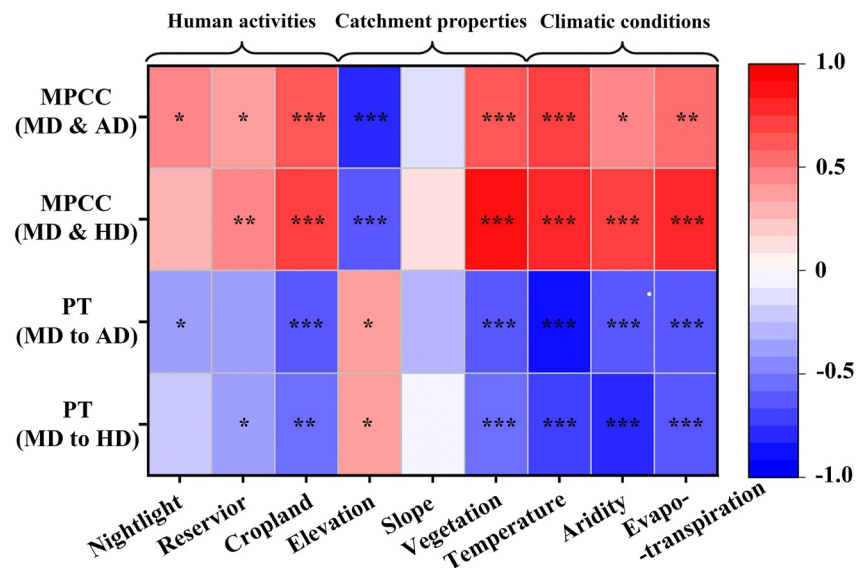


Figure 6. Heat map of the correlation coefficients. The horizontal axis represents the impact factors, including human activities (nightlight, reservoir, and cropland), catchment characteristics (elevation, slope, and vegetation), and climatic conditions (temperature, aridity, and evapotranspiration). The vertical axis represents the propagation time from meteorological drought to agricultural drought and hydrological drought and the maximum Pearson correlation coefficient between various types of droughts. The red colors indicate a positive correlation, and the blue colors indicate a negative correlation. The darker the color, the stronger the correlation. * represents the significance level $p < 0.05$, ** represents $p < 0.01$, *** represents $p < 0.001$.

4.3. The Correlation Between the Drought Propagation Time and Different Factors

The distribution of various factors exhibited high spatial heterogeneity due to the wide coverage in China (Figure S1 in Supporting Information S1). The correlation between different factors and PT varied dramatically (Figures 6 and 7, Tables S2 and S3 in Supporting Information S1), which demonstrates the various effects of potential factors on the process of drought propagation. The correlation between climatic factors and PT was the closest among the three types of indicators (Figure 6), which can explain 52.6% and 63.3% of the spatial variations in PT from meteorological to agricultural and hydrological droughts (Figure 7). In addition, catchment characteristics and human activities were also connected to the PT and relationships between droughts to some extent.

As for the propagation from meteorological to AD, temperature, aridity, and evapotranspiration contributed to 25.4%, 13.0%, and 14.2% of the PT, respectively (Figure 7a). Temperature was closely associated with PT ($R = -0.84$ and $p < 0.001$) and the relationship ($R = 0.74$ and $p < 0.001$). There were significant correlations between aridity and PT ($R = -0.60$ and $p < 0.001$) and the relationship ($R = 0.44$ and $p < 0.05$). The correlation coefficient between evapotranspiration and drought PT was -0.63 ($p < 0.001$). Human activities explained 24.2% of the variance in the PT from meteorological to agricultural droughts in China. The percentage of cropland contributed the most (14.4%) to spatial difference, which was strongly correlated with the PT ($R = -0.63$ and $p < 0.001$) and relationship ($R = 0.63$ and $p < 0.001$). Catchment characteristics explained 23.3% of the spatial difference in PT in China. Elevation was closely connected to the propagation relationship ($R = -0.78$ and $p < 0.001$). And there was also a relatively significant correlation between NDVI and PT ($R = -0.64$ and $p < 0.01$) and the relationship ($R = 0.59$ and $p < 0.001$),

As for the propagation from meteorological to HD, temperature, aridity, and evapotranspiration played a dominant role in the propagation, which contributed to 22.2%, 23.5%, and 17.6% of the divergence in the propagation process (Figure 7b), respectively. Temperature showed exceedingly significant correlations with PT ($R = -0.75$ and $p < 0.001$) and the propagation relationship ($R = 0.75$ and $p < 0.001$). Aridity was also considerably related to the PT and the relationship, with correlation coefficients of -0.77 and 0.71 ($p < 0.001$), respectively. There were also high correlation coefficients between evapotranspiration and the PT ($R = -0.66$ and $p < 0.001$) and the relationship ($R = 0.81$ and $p < 0.001$). Human activities only explained 18.3% of the variance in PT in China, where the contribution of cropland accounted for over 10% with correlation coefficients of -0.53 ($p < 0.01$).

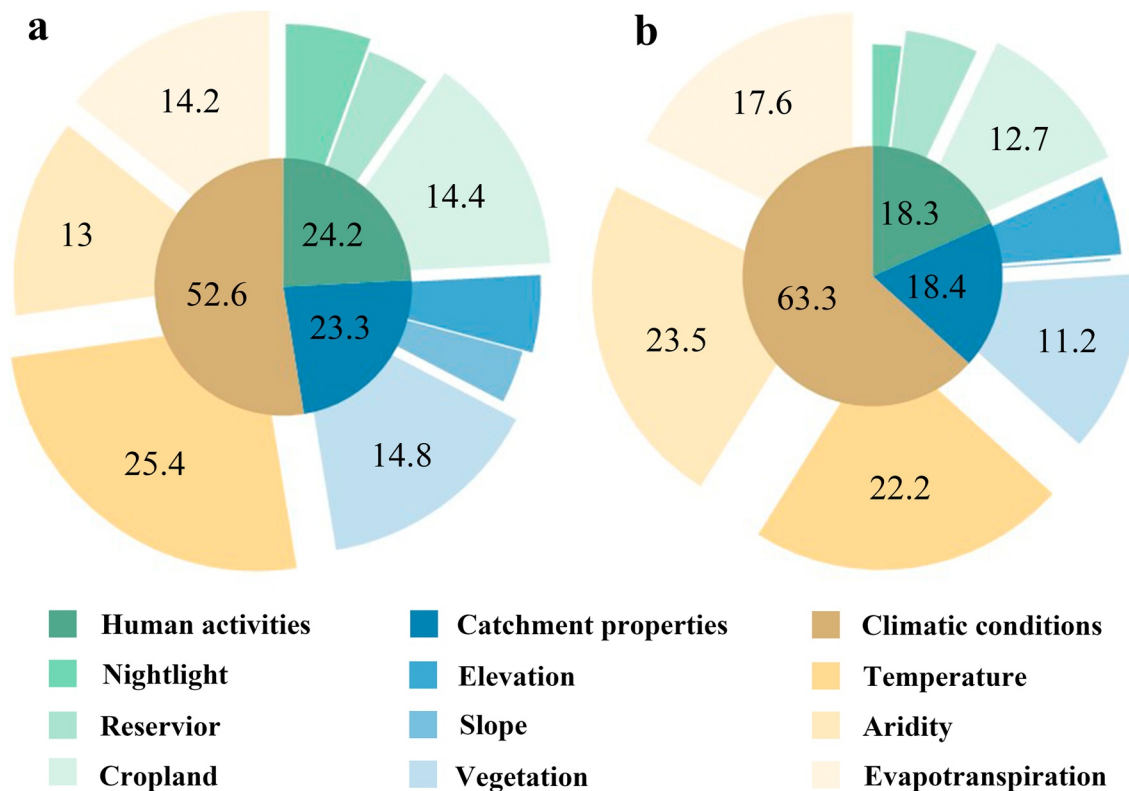


Figure 7. The contribution of all factors to the propagation time from meteorological to (a) agricultural and (b) hydrological drought. There are three kinds of factors: human activities (nightlight, reservoir, and cropland), catchment characteristics (elevation, slope, and vegetation), and climatic conditions (temperature, aridity, and evapotranspiration).

The correlation coefficients between reservoir and the PT ($R = -0.36$ and $p < 0.05$) and relationship ($R = 0.47$ and $p < 0.01$) were relatively low. The propagation from meteorological to hydrological droughts was also attributed to the catchment characteristics, with a total contribution of 18.4%. The contribution of elevation was approximately 6%, and the correlation coefficients with the PT and relationship were 0.37 ($p < 0.05$) and -0.6 ($p < 0.001$). Vegetation cover was also closely associated with the PT ($R = -0.56$ and $p < 0.001$) and relationships ($R = 0.85$ and $p < 0.001$).

5. Discussion

5.1. Validation of Results

In order to validate the results of this study and further demonstrate the impact of selected factors on the propagation from MD to agricultural and hydrological droughts, a more refined municipal division mode was adopted (as shown in Figure S9 of Supporting Information S1). This division paradigm was based on municipal regions and allowed us a larger amount of data, thus reducing the impact of spatial heterogeneity and enhancing the accuracy and reliability of the results. Based on the new division mode, we imported the generalized additive model (GAM) to fit the complicated non-linear relationships between selected indicators and the PT (Kim et al., 2019; Koch et al., 2022; Peng et al., 2023). Then we further explored the effects of various factors on drought propagation and the interaction between these factors from a spatial perspective by applying the geographic detector (GD) method (Luo et al., 2016; J. F. Wang et al., 2010). The detailed descriptions of these two methods are presented in Texts S3 and S4 of Supporting Information S1. Last, considering the significant influence of climatic conditions on drought propagation, we revealed the distribution and variance of drought PT under different climatic conditions.

5.1.1. The Non-Linear Relationships Between the Propagation Time and Various Factors

Figures 8 and 9 indicate the non-linear relationships between the drought PT and driving factors fitted by the GAM. Compared to the PCC method, the GAM can obtain a more complicated association between two variables.

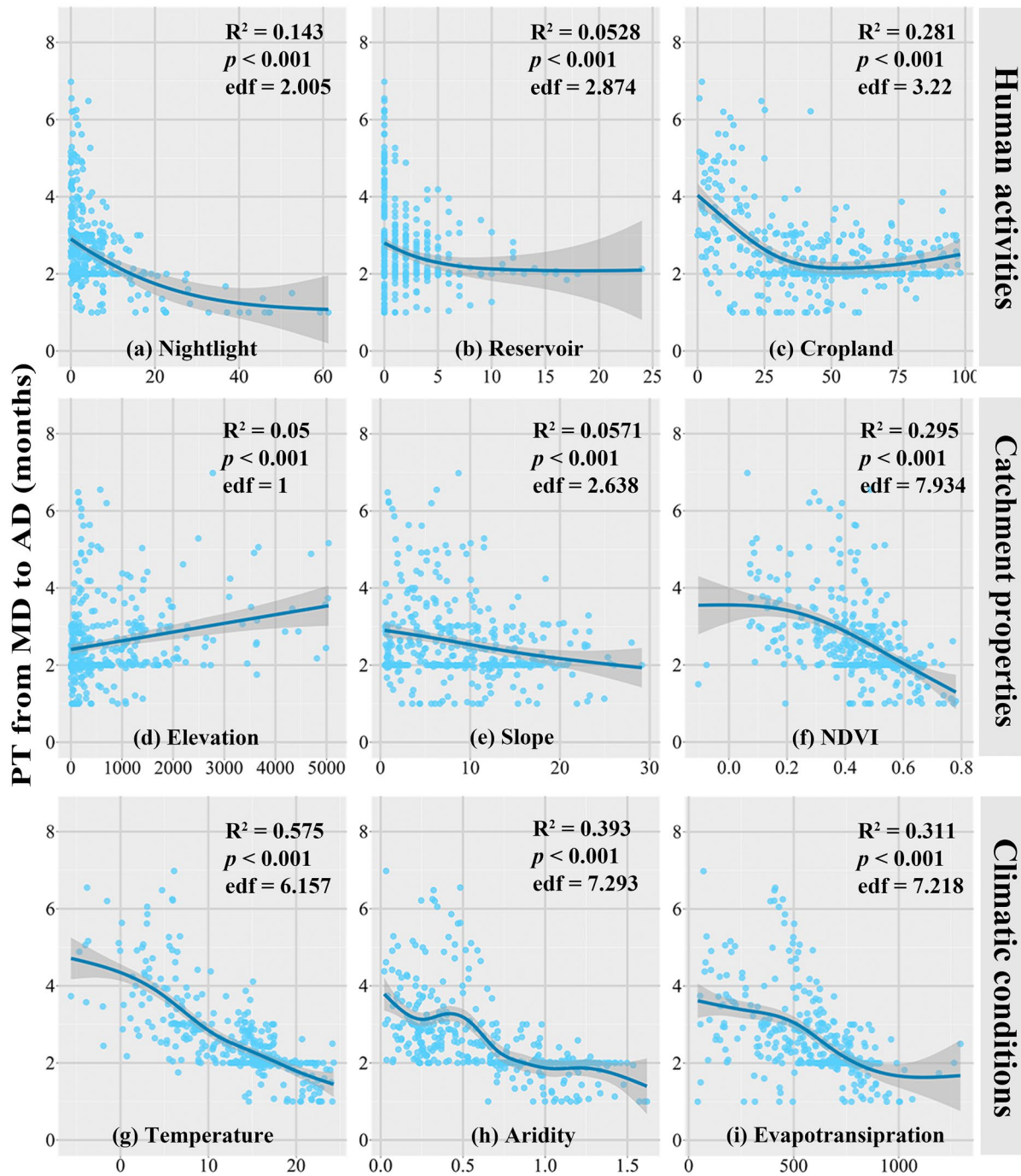


Figure 8. The non-linear relationship between the propagation time from meteorological drought to agricultural drought and nine factors, including (a) nightlight, (b) reservoir, (c) cropland, (d) elevation, (e) slope, (f) normalized difference vegetation index, (g) temperature, (h) aridity, and (i) evapotranspiration. The coefficient of determination (R^2), significance (p -value), and effective degrees of freedom (edf) of fitted functions are shown in the figure. The gray shaded area indicates the 95% confidence interval.

According to the coefficient of determination (R^2) and significance value (p) marked in the figures, we concluded that drought propagation was not determined by a single factor. Different indicators played various roles in the process of propagation from MD to AD and HD.

Furthermore, the outcomes of the GAM show significant similarity to that of the PCC. Climatic conditions were the most tightly connected to the PT from meteorological droughts to agricultural and hydrological droughts. For

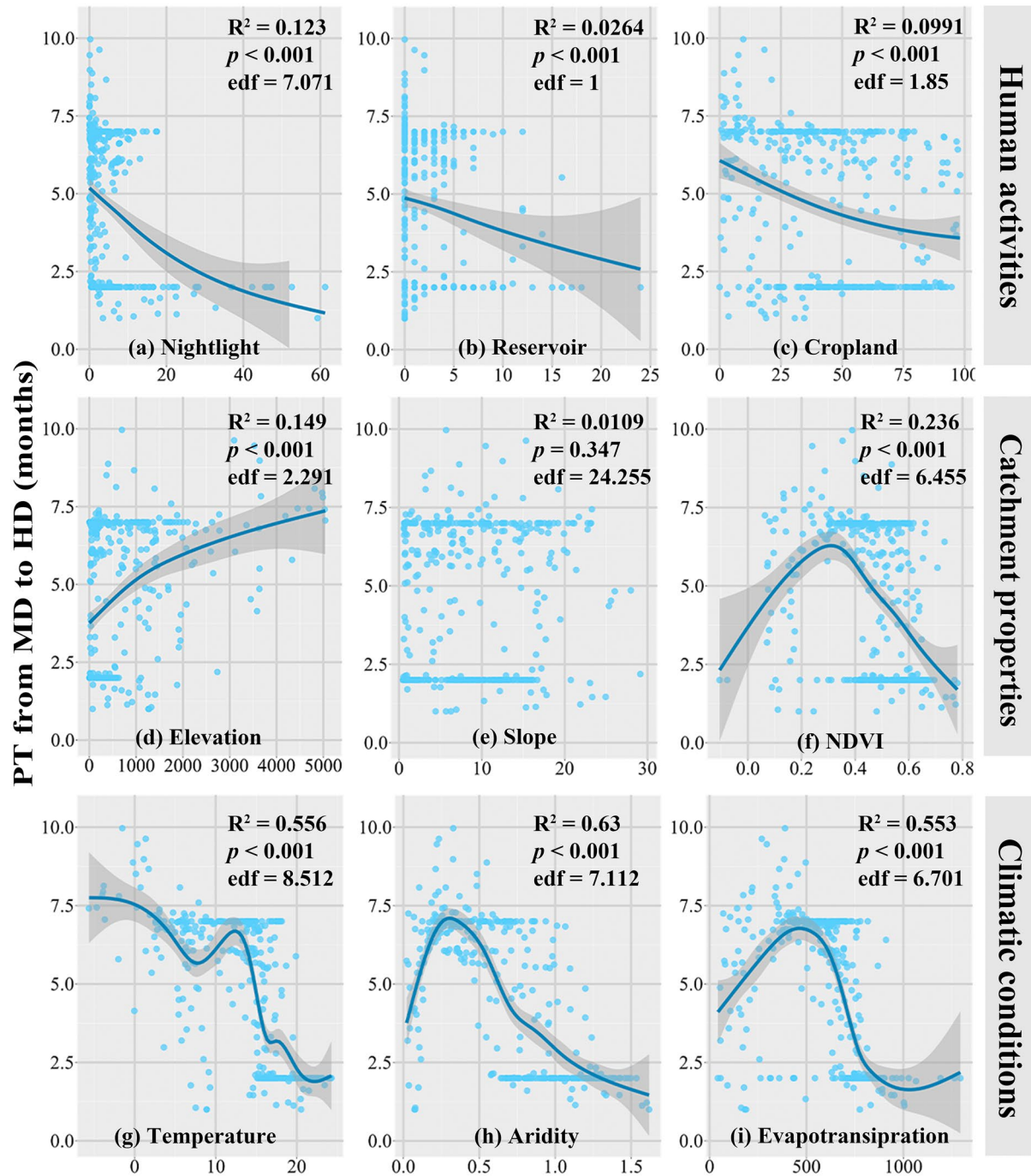


Figure 9. The non-linear relationship between the propagation time from meteorological drought to hydrological drought and nine factors, including (a) nightlight, (b) reservoir, (c) cropland, (d) elevation, (e) slope, (f) normalized difference vegetation index, (g) temperature, (h) aridity, and (i) evapotranspiration. The coefficient of determination (R^2), significance (p -value), and effective degrees of freedom (edf) of fitted functions are shown in the figure. The gray shaded area indicates the 95% confidence interval.

example, the temperature was closely related to the propagation from MD to AD ($R^2 = 0.575$, $p < 0.001$) and HD ($R^2 = 0.556$, $p < 0.001$), indicating that temperature considerably impacted the process of drought propagation. Aridity and evapotranspiration were also connected to the drought PT, especially the propagation from meteorological to HD ($R^2 > 0.5$, $p < 0.001$). In addition, the effects of vegetation cover and agricultural activities on drought spread also need to be taken into consideration in some areas.

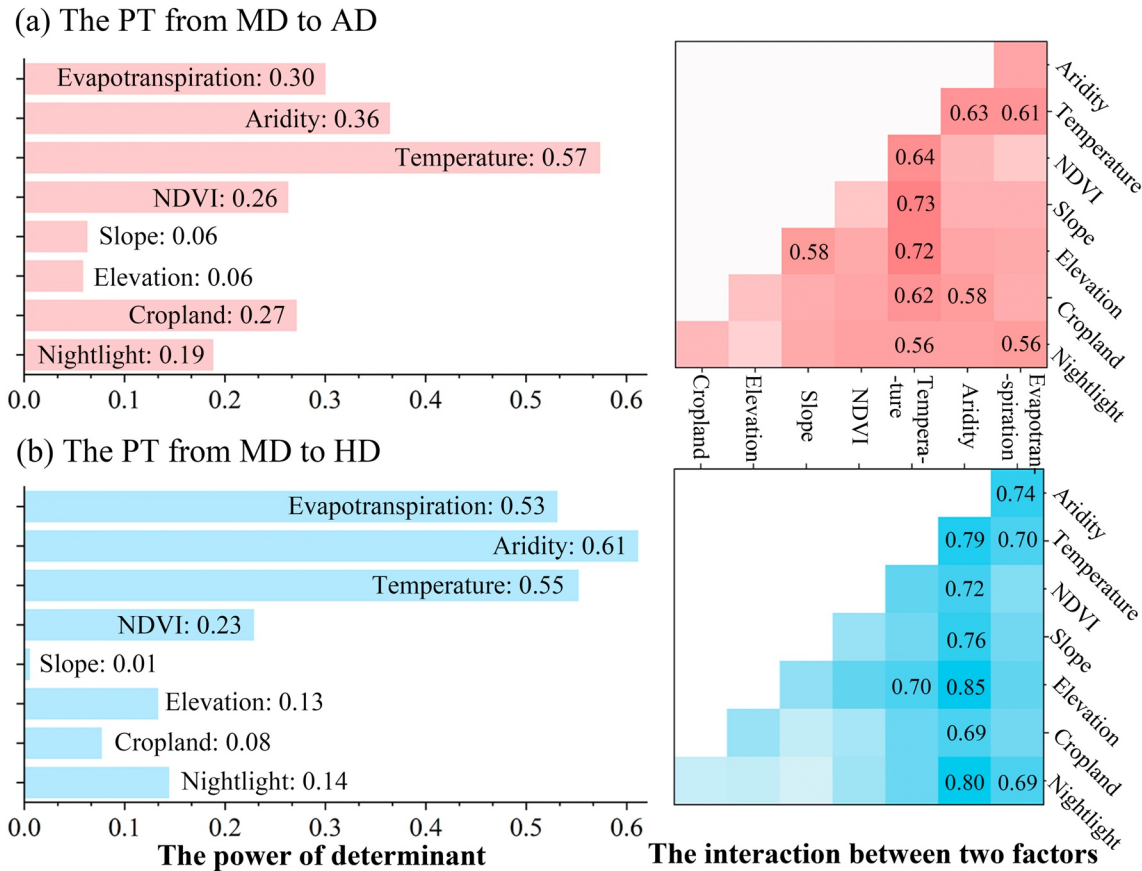


Figure 10. The power of determinant of various factors on the drought propagation time from meteorological drought to agricultural drought (AD, a) and hydrological drought (HD, b) and the interaction between two factors.

5.1.2. The Influencing Power of Various Factors and the Interaction Between Factors

According to the power of determinant and interaction captured by the GD, we can distinguish the impact of various factors on drought propagation and the interaction between each two indicators from a spatial perspective (Figure 10). The results revealed that there were huge differences in the explanatory power of various factors on the drought PT. Climatic conditions explained the most spatial differences in the drought PT and significantly interacted with other factors. In the meantime, it is worth noting that the results obtained by the GD do not differ much from the contributions calculated by the variance decomposition method, which reaffirms the accuracy and reliability of previous results in this study.

When it first comes to the propagation from meteorological to AD, we can tell that temperature had the strongest explanatory power for the PT (0.57), which was much higher than other factors. Aridity and evapotranspiration were the second and third most vital factors in the spread from MD to AD, with an explanatory degree of 0.36 and 0.3, respectively. In addition, NDVI and cropland also influenced the process of drought propagation. There were obvious interactions between different factors, especially climatic indicators. The interaction between two factors tended to impact drought propagation differently. For example, the explanatory power of temperature and aridity on the PT was bi-enhanced due to the interactions between them.

As for the propagation from meteorological to HD, aridity, temperature, and evapotranspiration were the three most crucial factors, with an explanatory power of 0.61, 0.55, and 0.53, respectively. Vegetation also affected the propagation process to some extent (0.23). There were more significant interactions between these factors, particularly aridity. For instance, the interaction between aridity and elevation was the most dominant (0.85) in the propagation from meteorological to HD, which nonlinearly enhanced the impact of each other on the propagation.

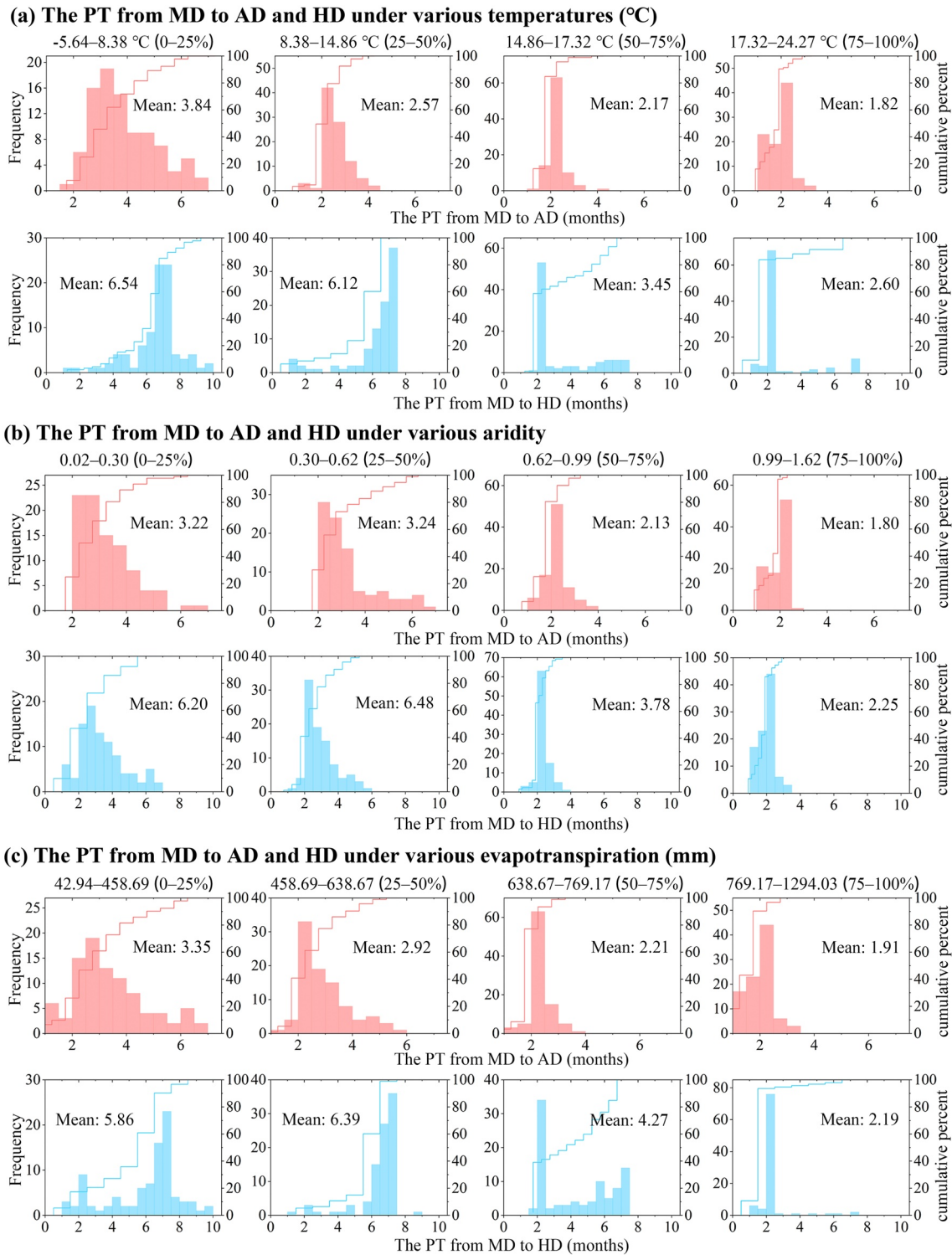


Figure 11. The distribution of the propagation time from meteorological drought to agricultural drought and hydrological drought under various climatic conditions (0%–25%, 25%–50%, 50%–75%, and 75%–100%), including (a) temperature, (b) aridity, and (c) evapotranspiration.

5.1.3. The Distribution of the Drought Propagation Time Under Various Climatic Conditions

Figure 11 shows the distribution and variance of the PT from meteorological to agricultural and hydrological droughts under various climatic conditions by the 25th percentile. According to Figure 11, obvious changes in the

PT were noticed with climate changes, which verified the vital impact of climatic conditions. When temperatures were relatively lower, the PT from meteorological droughts to agricultural and hydrological droughts was longer. As temperatures gradually increased, the propagation speed accelerated in most areas. The distribution of the PT under different aridity and evapotranspiration changed with the same trends (Figures 11b and 11c).

5.2. The Potential Causes Affecting Drought Propagation

In this study, we systematically discussed the influence of three kinds of factors (climatic conditions, human activities, and catchment characteristics) on drought propagation. The results showed that climatic conditions were the major factors affecting the propagation from meteorological to agricultural and hydrological droughts in China. Temperature and evapotranspiration had a crucial influence on drought propagation and these two factors were directly connected. High temperatures led to a decrease in the surface runoff and low soil moisture by directly increasing evapotranspiration from open surface water bodies and soil water and increasing groundwater consumption from vegetation transpiration when meteorological droughts occurred (Huang et al., 2017; D. Wang et al., 2011; M. Wang et al., 2021; T. Wang et al., 2021). Additionally, the scares in soil moisture caused by continuous temperature anomalies further absorbed surface water and groundwater, and thus triggered hydrological droughts (West et al., 2019). Therefore, the high temperature and strong evapotranspiration would shorten the PT from meteorological to agricultural and hydrological droughts, and enhance the linkage between different types of droughts (Huang et al., 2015; Ma et al., 2019). By contrast, low temperatures can turn rain into snow or ice, which is difficult to infiltrate into the soil (Van Loon et al., 2014; Xu et al., 2021); therefore, the response time of agricultural droughts to meteorological droughts would be extended. For example, in the region V and region I, the propagation speed was relatively low (4–8 months) because snow and ice were covered there, especially in winter. Aridity also affected the propagation from meteorological to agricultural and hydrological droughts (Gevaert et al., 2018). Compared to dry areas (region IV and I), meteorological droughts caused by a precipitation deficit were more likely to bring about a deficiency in surface runoff in humid climate zones (region VII and VIII), which we infer that it might be due to the greater sensitivity of agricultural and hydrological droughts to MD caused by rapid water cycle in humid regions (Xu et al., 2021). Simultaneously, these areas showed a stronger association between meteorological and hydrological droughts (Ding, Xu, et al., 2021; Haslinger et al., 2014).

In addition, human activities also affected the PT and relationships between droughts to some extent by regulating the hydrological process to modulate the response mechanism of agricultural and hydrological droughts to MD through the extraction of surface water and groundwater, construction of reservoirs and dams, agricultural irrigation, and development of cities (van Loon, 2013; Van Loon et al., 2016). Population growth and urbanization mainly regulated the propagation process of meteorological to agricultural droughts. Owing to the reduced infiltration rate of precipitation caused by large impervious areas, the deficiency in soil moisture would be accelerated when the continuous deficiency of precipitation occurred. Reservoir operation impacted the propagation relationship between meteorological and hydrological droughts by altering surface water exchange and hydrological cycles (Fang et al., 2020; J. Wu et al., 2016, 2017). The PT was shortened and the linkage between droughts was strengthened in areas with more reservoirs and dams, such as in regions VII, VIII, and IX. However, because of the seasonal regulation of reservoirs (Xing et al., 2021) which was not considered in this study, the correlation coefficients with the PT and relationship were relatively low. Compared to HD, the regulation of dams and reservoirs had a relatively weak impact on AD. However, some studies have also revealed that the construction of the Three Gorges Reservoir accelerated the propagation from meteorological to agricultural droughts in the Yangtze River Basin (Huang et al., 2021). The percentage of cropland was also an important factor affecting the propagation from meteorological to agricultural and hydrological droughts. Strong agricultural irrigation and production have accelerated the propagation process by reducing the flow of surface water and groundwater because of the intense utilization of water resources for crop growth (Ma et al., 2019). Intense agricultural production activities not only consumed large amounts of surface water and groundwater but also decreased the soil water content when precipitation did not meet the crop growth. Therefore, MD was more rapid in triggering an AD in these regions with stronger agricultural activities, such as in regions II, VII, VIII, and IX.

The propagation relationship between meteorological and agricultural and hydrological droughts was also affected by catchment characteristics (Z. Wu et al., 2015). The slope had little impact on the propagation from meteorological to agricultural and hydrological droughts from a large scale. Elevation had a key effect on the propagation from meteorological to agricultural droughts (van Loon, 2013). There was a longer response time

and a weaker linkage between meteorological and hydrological droughts in higher altitude areas (region V), which might be related to the wide coverage of immobile snow and ice blocking the hydrological cycles there (Van Loon et al., 2012). Widely covered snow, ice, and permafrost were difficult to lose or infiltrated into the ground in high-altitude regions (Van Loon, 2015); therefore, MD was less likely to propagate to AD in these areas. Vegetation cover dramatically affected the response of agricultural and hydrological droughts to MD (Huang et al., 2015). During drought periods, more vegetation consumed more soil water via transpiration, leading to a rapid deficiency in soil moisture (Guo et al., 2020; Han et al., 2019). When the precipitation decreased, the linkage between droughts was strengthened in areas of high vegetation cover because of a further decrease in water content due to intense transpiration and absorption (T. Zhang et al., 2022).

5.3. Implications and Limitations

5.3.1. Implications

Drought is the costliest natural disaster in the world (Hao et al., 2014), and could result in huge socio-economic losses and serious ecological problems. Therefore, it is very important to effectively prevent and manage droughts by developing suitable water resource strategies, where accurate drought prediction plays a key role. There are three key points in drought prediction: predictors, methods, and outputs (Mishra & Singh, 2011). The selection of predictors plays a predominant role in the accuracy of drought predictions. Hydrometeorological variables (e.g., precipitation and air temperature), corresponding drought indices, and large-scale meteorological indices (e.g., sea surface temperature) are the most common predictors (Hao et al., 2016). In this study, we revealed that there were high correlations between meteorological, agricultural, and hydrological droughts in most regions of China (see Section 4.3). Therefore, MD information can be considered a predictor when forecasting agricultural and hydrological droughts. The predictive ability of meteorological droughts for agricultural and hydrological droughts has been confirmed in some previous studies (Hao et al., 2016; Maity et al., 2016; Zhu et al., 2016). We also found that meteorological droughts could trigger agricultural and hydrological droughts in most of the studied areas; therefore, the drought PT could also be regarded as an input to predict agricultural and hydrological droughts based on accumulated precipitation deficiency. By analyzing the factors influencing drought propagation, we could accurately assess the PT for early agricultural and HD warnings when MD occurred, then the policy for drought management and prevention can be proposed to mitigate the losses caused by agricultural and hydrological droughts.

5.3.2. Limitations

There are several limitations of the data sets used in this study, which might cause uncertainties in the results. First, we selected a variety of data for the calculation of SPI, SSMI, and SRI, including precipitation from GPCC v.2020, soil moisture from GLDAS Noah LST L4, and runoff from GRUN, respectively. These data are from different institutions and present different properties (Table 2). Although these data sets were generated based on different models and methods and discrepancies between predicted and actual values are inevitable, they exemplify good spatio-temporal continuity and are widely used in previous studies (Golian et al., 2019; Y. Liu et al., 2019; Shi et al., 2022; Y. Zhang et al., 2021), confirming their merit and reasonable accuracy in research. In addition to the data sets obtained to calculate the SPI, SSMI, and SRI, the data driving the analysis of the causes of drought propagation showed a diversity of types and attributes. And as some data sets could not fully cover the years 1982–2014, we selected only those years for which data were available, which may also result in bias to the results.

6. Conclusions

In this study, the characteristics of meteorological, agricultural, and hydrological droughts in China during 1982–2014 were revealed based on the trends, number, duration, intensity, and severity. There are obvious spatial differences in the characteristics of these three types of droughts. The overall trend of MD was relatively insignificant compared to agricultural and HD. The incidence of AD events decreased in the west but increased in the northeast and central regions. Most regions experienced a hydrologically drying process, so we need to mainly focus on HD and mitigated its damages in the future.

The PT from meteorological to agricultural and hydrological droughts was calculated. We found that drought propagation exhibited high spatial heterogeneity in China, which was affected by a complex combination of

factors. Then we discussed the driving forces of drought propagation from three aspects: human activities, catchment characteristics, and climatic conditions. The results showed that temperature, evapotranspiration, aridity, and vegetation had more important impacts on drought propagation than other factors. High temperatures and strong evapotranspiration led to a decrease in surface runoff and low soil moisture and an increase in groundwater consumption from vegetation transpiration, which accelerated the propagation in southeast China (1–2 months). In addition, due to the insensitivity of runoff and soil moisture to precipitation deficits caused by slow water cycles in dry regions (northeast China), the PT was longer than in humid areas. Vegetation cover also dramatically affected the propagation process, agricultural and hydrological droughts will occur rapidly due to intense transpiration and absorption in high vegetation-covered areas.

Based on these findings, we will obtain supportive information for evaluating the dynamics of extreme drought events in the future and understanding the interactions between different types of droughts, which will play an important role in the prediction, warning, and management of different droughts. For example, the predictive capability of drought events (especially agricultural and hydrological droughts) will be strengthened by inputting the PT, potential affecting causes and MD information into prediction models. In addition, when regional MD occurred, the policy for alleviating the agricultural and hydrological droughts can be come up with in advance considering the PT and affecting causes, such as the operation of dam and the management of agricultural production.

Data Availability Statement

The subregion data of China were collected from the Resource and Environment Science and Data Center (RESDC, <https://www.resdc.cn/>). The precipitation, runoff, and soil moisture data used to calculate the SPI, SRI, and SSMI were obtained from the 0.5° Full Data Monthly Product of the Global Precipitation Climatology Centre (GPCC, Schneider et al., 2020, <https://opendata.dwd.de/>), the 0.5° Global Runoff Reconstruction data set (GRUN, Ghiggi et al., 2019, https://figshare.com/articles/dataset/GRUN_Global_Runoff_Reconstruction/9228176), and the 0.25° GLDAS version 2.0 Noah LSM L4 monthly data set (Beaudoin & Rodell, 2020; Rodell et al., 2004, <https://disc.gsfc.nasa.gov/>), respectively. Nightlight information (Defense Meteorological Satellite Program-Operational Linescan System (DMSP-OLS, Baugh et al., 2010) Nighttime Lights Time Series), the reservoir data, and the cropland information were collected from the RESDC (<https://www.resdc.cn/>), the Global Reservoir and Dam Database (GRanD, Lehner et al., 2011, <https://www.globaldamwatch.org/grand>), and the European Space Agency (ESA, 2017) Climate Change Initiative (CCI, Defourny et al., 2012, <https://www.esa-landcover-cci.org/>), respectively. The Elevation and slope data were provided by the Google Earth Engine platform (Jarvis et al., 2008, <https://code.earthengine.google.com/>). The NDVI data of the Global Inventory Monitoring and Modeling System (GIMM) were provided by NASA (<https://www.nasa.gov/nex>) and collected from the National Tibetan Plateau Third Pole Environment (TPDC, Pinzon & Tucker, 2014; Tucker et al., 2005; The National Center for Atmospheric Research, 2018, <https://data.tpdc.ac.cn/en/data/>). The air temperature, potential evapotranspiration, and actual evapotranspiration data were obtained from the 0.25° GLDAS version 2.0, Noah LSM L4 monthly data set (Beaudoin & Rodell, 2020; Rodell et al., 2004, <https://disc.gsfc.nasa.gov/>).

References

- Apurv, T., & Cai, X. (2020). Drought propagation in contiguous U.S. Watersheds: A process-based understanding of the role of climate and watershed properties. *Water Resources Research*, 56(9), e2020WR027755. <https://doi.org/10.1029/2020wr027755>
- Ayantobo, O. O., Li, Y., Song, S., & Yao, N. (2017). Spatial comparability of drought characteristics and related return periods in mainland China over 1961–2013. *Journal of Hydrology*, 550, 549–567. <https://doi.org/10.1016/j.jhydrol.2017.05.019>
- Bae, H., Ji, H., Lim, Y.-J., Ryu, Y., Kim, M.-H., & Kim, B.-J. (2019). Characteristics of drought propagation in South Korea: Relationship between meteorological, agricultural, and hydrological droughts. *Natural Hazards*, 99, 1–16. <https://doi.org/10.1007/s11069-019-03676-3>
- Barker, L. J., Hannaford, J., Chiverton, A., & Svensson, C. (2016). From meteorological to hydrological drought using standardised indicators. *Hydrology and Earth System Sciences*, 20(6), 2483–2505. <https://doi.org/10.5194/hess-20-2483-2016>
- Baugh, K., Elvidge, C. D., Ghosh, T., & Ziskin, D. (2010). Development of a 2009 stable lights product using DMSP-OLS data [Dataset]. Proceedings of the Asia-Pacific Advanced Network, 30, 114. <https://doi.org/10.7125/apan.30.17>
- Beaudoin, H., & Rodell, M. (2020). GLDAS Noah land surface model L4 monthly 0.25 x 0.25 degree V2.1 [Dataset]. Goddard Earth Sciences Data and Information Services Center. <https://doi.org/10.5067/9SQ1B3ZXP2C5>
- Becker, A., Finger, P., Meyer-Christoffer, A., Rudolf, B., Schamm, K., Schneider, U., & Ziese, M. (2013). A description of the global land-surface precipitation data products of the Global Precipitation Climatology Centre with sample applications including centennial (trend) analysis from 1901–present [Dataset]. Earth System Science Data, 5(1), 71–99. <https://doi.org/10.5194/essd-5-71-2013>
- Bevacqua, A. G., Chaffe, P. L. B., Chagas, V. B. P., & AghaKouchak, A. (2021). Spatial and temporal patterns of propagation from meteorological to hydrological droughts in Brazil. *Journal of Hydrology*, 603, 126902. <https://doi.org/10.1016/j.jhydrol.2021.126902>

Acknowledgments

This study was supported by the National Key Research and Development Program of China (no. 2022YFF0711603), the Fundamental Research Funds for the Central Universities (no. 0209-14380093, 0209-14380097), the Frontiers Science Center for Critical Earth Material Cycling Fund (JBGS2102), National Natural Science Foundation of China (no. 41671423), and the Ministry Science and Technology Development of China-Data Sharing Infrastructure of Earth System Science (no. 2005DKA32300).

- Bhardwaj, K., Shah, D., Aadhar, S., & Mishra, V. (2020). Propagation of meteorological to hydrological droughts in India. *Journal of Geophysical Research: Atmospheres*, 125(22), e2020JD033455. <https://doi.org/10.1029/2020jd033455>
- Chen, N., Li, R., Zhang, X., Yang, C., Wang, X., Zeng, L., et al. (2020). Drought propagation in northern China plain: A comparative analysis of GLDAS and MERRA-2 datasets. *Journal of Hydrology*, 588, 125026. <https://doi.org/10.1016/j.jhydrol.2020.125026>
- Dai, A. (2010). Drought under global warming: A review. *WIREs Climate Change*, 2(1), 45–65. <https://doi.org/10.1002/wcc.81>
- Dai, A. (2012). Increasing drought under global warming in observations and models. *Nature Climate Change*, 3(1), 52–58. <https://doi.org/10.1038/nclimate1633>
- Das, S., Das, J., & Umamahesh, N. V. (2022). Investigating the propagation of droughts under the influence of large-scale climate indices in India. *Journal of Hydrology*, 610, 127900. <https://doi.org/10.1016/j.jhydrol.2022.127900>
- Defourny, P., Kirches, G., Brockmann, C., Boettcher, M., Peters, M., Bontemps, S., et al. (2012). Land cover CCI [Dataset]. Product User Guide Version, 2. Retrieved from <http://www.gofcgold.wur.nl/>
- Ding, Y., Gong, X., Xing, Z., Cai, H., Zhou, Z., Zhang, D., et al. (2021). Attribution of meteorological, hydrological and agricultural drought propagation in different climatic regions of China. *Agricultural Water Management*, 255, 106996. <https://doi.org/10.1016/j.agwat.2021.106996>
- Ding, Y., Xu, J., Wang, X., Cai, H., Zhou, Z., Sun, Y., & Shi, H. (2021). Propagation of meteorological to hydrological drought for different climate regions in China. *Journal of Environmental Management*, 283, 111980. <https://doi.org/10.1016/j.jenvman.2021.111980>
- Douglas, E., Vogel, R., & Kroll, C. (2000). Trends in floods and low flows in the United States: Impact of spatial correlation. *Journal of Hydrology*, 240(1–2), 90–105. [https://doi.org/10.1016/S0022-1694\(00\)00336-X](https://doi.org/10.1016/S0022-1694(00)00336-X)
- European Space Agency. (2017). Land Cover CCI Product user guide version 2 (Technical Report).
- Fang, W., Huang, S., Huang, Q., Huang, G., Wang, H., Leng, G., & Wang, L. (2020). Identifying drought propagation by simultaneously considering linear and nonlinear dependence in the Wei River basin of the Loess Plateau, China. *Journal of Hydrology*, 591, 125287. <https://doi.org/10.1016/j.jhydrol.2020.125287>
- Gevaert, A. I., Veldkamp, T. I. E., & Ward, P. J. (2018). The effect of climate type on timescales of drought propagation in an ensemble of global hydrological models. *Hydrology and Earth System Sciences*, 22(9), 4649–4665. <https://doi.org/10.5194/hess-22-4649-2018>
- Ghiggi, G., Humphrey, V., Seneviratne, S. I., & Gudmundsson, L. (2019). GRUN: An observation-based global gridded runoff dataset from 1902 to 2014 [Dataset]. Earth System Science Data, 11(4), 1655–1674. <https://doi.org/10.5194/essd-11-1655-2019>
- Gocic, M., & Trajkovic, S. (2013). Analysis of changes in meteorological variables using Mann-Kendall and Sen's slope estimator statistical tests in Serbia. *Global and Planetary Change*, 100, 172–182. <https://doi.org/10.1016/j.gloplacha.2012.10.014>
- Golian, S., Javadian, M., & Behrangi, A. (2019). On the use of satellite, gauge, and reanalysis precipitation products for drought studies. *Environmental Research Letters*, 14(7), 075005. <https://doi.org/10.1088/1748-9326/ab2203>
- Greve, P., Roderick, M. L., Ukkola, A. M., & Wada, Y. (2019). The aridity Index under global warming. *Environmental Research Letters*, 14(12), 124006. <https://doi.org/10.1088/1748-9326/ab5046>
- Guo, Y., Huang, S., Huang, Q., Leng, G., Fang, W., Wang, L., & Wang, H. (2020). Propagation thresholds of meteorological drought for triggering hydrological drought at various levels. *Science of the Total Environment*, 712, 136502. <https://doi.org/10.1016/j.scitotenv.2020.136502>
- Guo, Y., Huang, S., Huang, Q., Wang, H., Fang, W., Yang, Y., & Wang, L. (2019a). Assessing socioeconomic drought based on an improved multivariate standardized reliability and resilience index. *Journal of Hydrology*, 568, 904–918. <https://doi.org/10.1016/j.jhydrol.2018.11.055>
- Guo, Y., Huang, S., Huang, Q., Wang, H., Wang, L., & Fang, W. (2019b). Copulas-based bivariate socioeconomic drought dynamic risk assessment in a changing environment. *Journal of Hydrology*, 575, 1052–1064. <https://doi.org/10.1016/j.jhydrol.2019.06.010>
- Han, Z., Huang, S., Huang, Q., Leng, G., Wang, H., Bai, Q., et al. (2019). Propagation dynamics from meteorological to groundwater drought and their possible influence factors. *Journal of Hydrology*, 578, 124102. <https://doi.org/10.1016/j.jhydrol.2019.124102>
- Hao, Z., AghaKouchak, A., Nakhjiri, N., & Farahmand, A. (2014). Global integrated drought monitoring and prediction system. *Scientific Data*, 1, 140001. <https://doi.org/10.1038/sdata.2014.1>
- Hao, Z., Hao, F., Singh, V. P., Ouyang, W., & Cheng, H. (2017). An integrated package for drought monitoring, prediction and analysis to aid drought modeling and assessment. *Environmental Modelling & Software*, 91, 199–209. <https://doi.org/10.1016/j.envsoft.2017.02.008>
- Hao, Z., Hao, F., Singh, V. P., Sun, A. Y., & Xia, Y. (2016). Probabilistic prediction of hydrologic drought using a conditional probability approach based on the meta-Gaussian model. *Journal of Hydrology*, 542, 772–780. <https://doi.org/10.1016/j.jhydrol.2016.09.048>
- Haslinger, K., Koffler, D., Schöner, W., & Laaha, G. (2014). Exploring the link between meteorological drought and streamflow: Effects of climate-catchment interaction. *Water Resources Research*, 50(3), 2468–2487. <https://doi.org/10.1002/2013wr015051>
- He, X., Pan, M., Wei, Z., Wood, E. F., & Sheffield, J. (2020). A global drought and flood catalogue from 1950 to 2016. *Bulletin of the American Meteorological Society*, 101(5), E508–E535. <https://doi.org/10.1175/bams-d-18-0269.1>
- Huang, S., Huang, Q., Chang, J., Leng, G., & Xing, L. (2015). The response of agricultural drought to meteorological drought and the influencing factors: A case study in the Wei River Basin, China. *Agricultural Water Management*, 159, 45–54. <https://doi.org/10.1016/j.agwat.2015.05.023>
- Huang, S., Li, P., Huang, Q., Leng, G., Hou, B., & Ma, L. (2017). The propagation from meteorological to hydrological drought and its potential influence factors. *Journal of Hydrology*, 547, 184–195. <https://doi.org/10.1016/j.jhydrol.2017.01.041>
- Huang, S., Zhang, X., Chen, N., Li, B., Ma, H., Xu, L., et al. (2021). Drought propagation modification after the construction of the three Gorges dam in the Yangtze River Basin. *Journal of Hydrology*, 603, 127138. <https://doi.org/10.1016/j.jhydrol.2021.127138>
- Jarvis, A., Reuter, H. I., Nelson, A., & Guevara, E. (2008). Hole-filled SRTM for the globe version 4. [Dataset]. CGIAR-CSI SRTM 90m Database, 15, 5. <http://srtm.csi.cgiar.org>
- Kendall, M. G. (1948). *Rank correlation methods*. Griffin.
- Kim, J. H., Lee, D. H., & Kang, J.-H. (2019). Associating the spatial properties of a watershed with downstream Chl-a concentration using spatial analysis and generalized additive models. *Water Research*, 154, 387–401. <https://doi.org/10.1016/j.watres.2019.02.010>
- Koch, J. C., Bogard, M. J., Butman, D. E., Finlay, K., Ebel, B., James, J., et al. (2022). Heterogeneous patterns of aged organic carbon export driven by hydrologic flow paths, soil texture, fire, and thaw in discontinuous permafrost headwaters. *Global Biogeochemical Cycles*, 36(4), e2021GB007242. <https://doi.org/10.1029/2021gb007242>
- Larkin, N. K., & Harrison, D. (2005). Global seasonal temperature and precipitation anomalies during El Niño autumn and winter. *Geophysical Research Letters*, 32(16), L16705. <https://doi.org/10.1029/2005gl022860>
- Lehner, B., Liermann, C. R., Revenga, C., Vörösmarty, C., Fekete, B., Crouzet, P., et al. (2011). High-resolution mapping of the world's reservoirs and dams for sustainable river-flow management. *Frontiers in Ecology and the Environment*, 9, 494–502. <https://doi.org/10.1890/100125>
- Leng, G., Tang, Q., & Rayburg, S. (2015). Climate change impacts on meteorological, agricultural and hydrological droughts in China. *Global and Planetary Change*, 126, 23–34. <https://doi.org/10.1016/j.gloplacha.2015.01.003>
- Li, R., Chen, N., Zhang, X., Zeng, L., Wang, X., Tang, S., et al. (2020). Quantitative analysis of agricultural drought propagation process in the Yangtze River Basin by using cross wavelet analysis and spatial autocorrelation. *Agricultural and Forest Meteorology*, 280, 107809. <https://doi.org/10.1016/j.agrformet.2019.107809>

- Lin, W., Wen, C., Wen, Z., & Gang, H. (2015). Drought in Southwest China: A review. *Atmospheric and Oceanic Science Letters*, 8, 339–344.
- Liu, S., Shi, H., & Sivakumar, B. (2020). Socioeconomic drought under growing population and changing climate: A new index considering the resilience of a regional water resources system. *Journal of Geophysical Research: Atmospheres*, 125(15), 1–21. <https://doi.org/10.1029/2020jd033005>
- Liu, Y., Liu, Y., & Wang, W. (2019). Inter-comparison of satellite-retrieved and Global Land Data Assimilation System-simulated soil moisture datasets for global drought analysis. *Remote Sensing of Environment*, 220, 1–18. <https://doi.org/10.1016/j.rse.2018.10.026>
- Long, D., Shen, Y. J., Sun, A. Y., Hong, Y., Longuevergne, L., Yang, Y. T., et al. (2014). Drought and flood monitoring for a large karst plateau in Southwest China using extended GRACE data. *Remote Sensing of Environment*, 155, 145–160. <https://doi.org/10.1016/j.rse.2014.08.006>
- Long, D., Yang, W., Scanlon, B. R., Zhao, J., Liu, D., Burek, P., et al. (2020). South-to-North Water Diversion stabilizing Beijing's groundwater levels. *Nature Communications*, 11(1), 3665. <https://doi.org/10.1038/s41467-020-17428-6>
- Loukas, A., & Vasilades, L. (2004). Probabilistic analysis of drought spatiotemporal characteristics in Thessaly region, Greece. *Natural Hazards and Earth System Sciences*, 4(5/6), 719–731. <https://doi.org/10.5194/nhess-4-719-2004>
- Luo, W., Sasiewicz, J., Stepinski, T., Wang, J., Xu, C., & Cang, X. (2016). Spatial association between dissection density and environmental factors over the entire conterminous United States. *Geophysical Research Letters*, 43(2), 692–700. <https://doi.org/10.1002/2015gl066941>
- Ma, F., Luo, L., Ye, A., & Duan, Q. (2019). Drought characteristics and propagation in the semiarid Heihe River Basin in northwestern China. *Journal of Hydrometeorology*, 20(1), 59–77. <https://doi.org/10.1175/jhm-d-18-0129.1>
- Maity, R., Suman, M., & Verma, N. K. (2016). Drought prediction using a wavelet based approach to model the temporal consequences of different types of droughts. *Journal of Hydrology*, 539, 417–428. <https://doi.org/10.1016/j.jhydrol.2016.05.042>
- Mann, H. B. (1945). Nonparametric tests against trend. *Econometrica: Journal of the Econometric Society*, 13(3), 245–259. <https://doi.org/10.2307/1907187>
- Martínez-Fernández, J., González-Zamora, A., Sánchez, N., Gumuzzio, A., & Herrero-Jiménez, C. M. (2016). Satellite soil moisture for agricultural drought monitoring: Assessment of the SMOS derived Soil Water Deficit Index. *Remote Sensing of Environment*, 177, 277–286. <https://doi.org/10.1016/j.rse.2016.02.064>
- Mason, S. J., & Goddard, L. (2001). Probabilistic precipitation anomalies associated with ENSO. *Bulletin of the American Meteorological Society*, 82(4), 619–638. [https://doi.org/10.1175/1520-0477\(2001\)082<0619:ppaawe>2.3.co;2](https://doi.org/10.1175/1520-0477(2001)082<0619:ppaawe>2.3.co;2)
- McKee, T. B., Doesken, N. J., & Kleist, J. (1993). The relationship of drought frequency and duration to time scales. *Proceedings of the 8th Conference on Applied Climatology*, 17(22), 179–183.
- Mishra, A. K., & Singh, V. P. (2010). A review of drought concepts. *Journal of Hydrology*, 391(1–2), 202–216. <https://doi.org/10.1016/j.jhydrol.2010.07.012>
- Mishra, A. K., & Singh, V. P. (2011). Drought modeling—A review. *Journal of Hydrology*, 403(1–2), 157–175. <https://doi.org/10.1016/j.jhydrol.2011.03.049>
- Nastos, P. T., Politi, N., & Kapsomenakis, J. (2013). Spatial and temporal variability of the aridity index in Greece. *Atmospheric Research*, 119, 140–152. <https://doi.org/10.1016/j.atmosres.2011.06.017>
- Palmer, W. C. (1965). *Meteorological drought*. US Department of Commerce, Weather Bureau.
- Palmer, W. C. (1968). Keeping track of crop moisture conditions, nationwide: The new crop moisture index. *Weatherwise*, 21(4), 156–161. <https://doi.org/10.1080/00431672.1968.9932814>
- Pearson, K. (1895). Notes on regression and inheritance in the case of two parents. *Proceedings of the Royal Society of London*, 58, 240–242.
- Peng, J., Hu, T., Qiu, S., Hu, Y. n., Dong, J., & Lin, Y. (2023). Balancing the effects of forest conservation and restoration on South China karst greening. *Earth's Future*, 11(6), e2023EF003487. <https://doi.org/10.1029/2023ef003487>
- Pinzon, J. E., & Tucker, C. J. (2014). A non-stationary 1981–2012 AVHRR NDVI3g time series. [Dataset]. *Remote Sensing*, 6(8), 6929–6960. <https://doi.org/10.3390/rs6086929>
- Rodell, M., Houser, P., Jambor, U., Gottschalk, J., Mitchell, K., Meng, C.-J., et al. (2004). The global land data assimilation system [Dataset]. *Bulletin of the American Meteorological Society*, 85(3), 381–394. <https://doi.org/10.1175/bams-85-3-381>
- Samaniego, L., Kumar, R., & Zink, M. (2013). Implications of parameter uncertainty on soil moisture drought analysis in Germany. *Journal of Hydrometeorology*, 14(1), 47–68. <https://doi.org/10.1175/jhm-d-12-075.1>
- Schneider, U., Becker, A., Finger, P., Rustemeier, E., & Ziese, M. (2020). GPCC full data monthly product version 2020 at 0.25°: Monthly land-surface precipitation from rain-gauges built on GTS-based and historical data [Dataset]. Global Precipitation Climatology Centre (GPCC) at Deutscher Wetterdienst. https://doi.org/10.5676/DWD_GPCC/FD_M_V2020_025
- Sen, P. K. (1968). Estimates of the regression coefficient based on Kendall's Tau. *Journal of the American Statistical Association*, 63(324), 1379–1389. <https://doi.org/10.1080/01621459.1968.10480934>
- Shen, Z., Zhang, Q., Singh, V. P., Sun, P., Song, C., & Yu, H. (2019). Agricultural drought monitoring across Inner Mongolia, China: Model development, spatiotemporal patterns and impacts. *Journal of Hydrology*, 571, 793–804. <https://doi.org/10.1016/j.jhydrol.2019.02.028>
- Shi, H., Chen, J., Wang, K., & Niu, J. (2018). A new method and a new index for identifying socioeconomic drought events under climate change: A case study of the East River Basin in China. *Science of the Total Environment*, 616–617, 363–375. <https://doi.org/10.1016/j.scitotenv.2017.10.321>
- Shi, H., Zhou, Z., Liu, L., & Liu, S. (2022). A global perspective on propagation from meteorological drought to hydrological drought during 1902–2014. *Atmospheric Research*, 280, 106441. <https://doi.org/10.1016/j.atmosres.2022.106441>
- Shukla, S., & Wood, A. W. (2008). Use of a standardized runoff index for characterizing hydrologic drought. *Geophysical Research Letters*, 35(2), L02405. <https://doi.org/10.1029/2007gl032487>
- Spinoni, J., Naumann, G., Carrao, H., Barbosa, P., & Vogt, J. (2014). World drought frequency, duration, and severity for 1951–2010. *International Journal of Climatology*, 34(8), 2792–2804. <https://doi.org/10.1002/joc.3875>
- Stahl, K., & Heudorfer, B. (2017). Comparison of different threshold level methods for drought propagation analysis in Germany. *Hydrology Research*, 48(5), 1311–1326. <https://doi.org/10.2166/nh.2016.258>
- Sun, Q., Miao, C., Duan, Q., Ashouri, H., Sorooshian, S., & Hsu, K. L. (2018). A review of global precipitation data sets: Data sources, estimation, and intercomparisons. *Reviews of Geophysics*, 56(1), 79–107. <https://doi.org/10.1002/2017rg000574>
- Tabari, H., Marofi, S., Aeni, A., Talaei, P. H., & Mohammadi, K. (2011). Trend analysis of reference evapotranspiration in the western half of Iran. *Agricultural and Forest Meteorology*, 151(2), 128–136. <https://doi.org/10.1016/j.agrformet.2010.09.009>
- The National Center for Atmospheric Research. (2018). Global GIMMS NDVI3g v1 dataset (1981–2015) [Dataset]. A Big Earth Data Platform for Three Poles. <https://poles.tpdc.ac.cn/en/data/9775f2b4-7370-4e5e-a537-3482c9a83d88/>
- Tijdeman, E., Barker, L. J., Svoboda, M. D., & Stahl, K. (2018). Natural and human influences on the link between meteorological and hydrological drought indices for a large set of catchments in the contiguous United States. *Water Resources Research*, 54(9), 6005–6023. <https://doi.org/10.1029/2017wr022412>

- Tu, X., Wu, H., Singh, V. P., Chen, X., Lin, K., & Xie, Y. (2018). Multivariate design of socioeconomic drought and impact of water reservoirs. *Journal of Hydrology*, 566, 192–204. <https://doi.org/10.1016/j.jhydrol.2018.09.012>
- Tucker, C. J., Pinzon, J. E., Brown, M. E., Slayback, D. A., Pak, E. W., Mahoney, R., et al. (2005). An extended AVHRR 8-km NDVI dataset compatible with MODIS and SPOT vegetation NDVI data [Dataset]. *International Journal of Remote Sensing*, 26(20), 4485–4498. <https://doi.org/10.1080/01431160500168686>
- van Loon, A. F. (2013). *On the propagation of drought: How climate and catchment characteristics influence hydrological drought development and recovery*. Wageningen University and Research.
- Van Loon, A. F. (2015). Hydrological drought explained. *WIREs Water*, 2(4), 359–392. <https://doi.org/10.1002/wat2.1085>
- Van Loon, A. F., Gleeson, T., Clark, J., Van Dijk, A. I. J. M., Stahl, K., Hannaford, J., et al. (2016). Drought in the Anthropocene. *Nature Geoscience*, 9(2), 89–91. <https://doi.org/10.1038/ngeo2646>
- Van Loon, A. F., & Laaha, G. (2015). Hydrological drought severity explained by climate and catchment characteristics. *Journal of Hydrology*, 526, 3–14. <https://doi.org/10.1016/j.jhydrol.2014.10.059>
- Van Loon, A. F., Tjiedeman, E., Wanders, N., Van Lanen, H. A. J., Teuling, A. J., & Uijlenhoet, R. (2014). How climate seasonality modifies drought duration and deficit. *Journal of Geophysical Research: Atmospheres*, 119(8), 4640–4656. <https://doi.org/10.1002/2013jd020383>
- Van Loon, A. F., Van Huijgevoort, M. H. J., & Van Lanen, H. A. J. (2012). Evaluation of drought propagation in an ensemble mean of large-scale hydrological models. *Hydrology and Earth System Sciences*, 16(11), 4057–4078. <https://doi.org/10.5194/hess-16-4057-2012>
- Vicente-Serrano, S. M., López-Moreno, J. I., Beguería, S., Lorenzo-Lacruz, J., Azorin-Molina, C., & Morán-Tejada, E. (2012). Accurate computation of a streamflow drought index. *Journal of Hydrologic Engineering*, 17(2), 318–332. [https://doi.org/10.1061/\(asce\)jhe.1943-5584.0000433](https://doi.org/10.1061/(asce)jhe.1943-5584.0000433)
- Wang, D., Hejazi, M., Cai, X., & Valocchi, A. J. (2011). Climate change impact on meteorological, agricultural, and hydrological drought in central Illinois. *Water Resources Research*, 47(9), W09527. <https://doi.org/10.1029/2010wr009845>
- Wang, F., Lai, H., Li, Y., Feng, K., Zhang, Z., Tian, Q., et al. (2022). Dynamic variation of meteorological drought and its relationships with agricultural drought across China. *Agricultural Water Management*, 261, 107301. <https://doi.org/10.1016/j.agwat.2021.107301>
- Wang, J. F., Li, X. H., Christakos, G., Liao, Y. L., Zhang, T., Gu, X., & Zheng, X. Y. (2010). Geographical detectors-based health risk assessment and its application in the neural tube defects study of the Heshun Region, China. *International Journal of Geographical Information Science*, 24(1), 107–127. <https://doi.org/10.1080/13658810802443457>
- Wang, M., Jiang, S., Ren, L., Xu, C.-Y., Menzel, L., Yuan, F., et al. (2021). Separating the effects of climate change and human activities on drought propagation via a natural and human-impacted catchment comparison method. *Journal of Hydrology*, 603, 126913. <https://doi.org/10.1016/j.jhydrol.2021.126913>
- Wang, T., Tu, X., Singh, V. P., Chen, X., & Lin, K. (2021). Global data assessment and analysis of drought characteristics based on CMIP6. *Journal of Hydrology*, 596, 126091. <https://doi.org/10.1016/j.jhydrol.2021.126091>
- Wang, W., Ertsen, M. W., Svoboda, M. D., & Hafeez, M. (2016). Propagation of drought: From meteorological drought to agricultural and hydrological drought. *Advances in Meteorology*, 2016, 1–5. <https://doi.org/10.1155/2016/6547209>
- Wang, Y., Wang, S., Li, G., Zhang, H., Jin, L., Su, Y., & Wu, K. (2017). Identifying the determinants of housing prices in China using spatial regression and the geographical detector technique. *Applied Geography*, 79, 26–36. <https://doi.org/10.1016/j.apgeog.2016.12.003>
- Wang, Z., Li, J., Lai, C., Zeng, Z., Zhong, R., Chen, X., et al. (2017). Does drought in China show a significant decreasing trend from 1961 to 2009? *Science of the Total Environment*, 579, 314–324. <https://doi.org/10.1016/j.scitotenv.2016.11.098>
- West, H., Quinn, N., & Horswell, M. (2019). Remote sensing for drought monitoring & impact assessment: Progress, past challenges and future opportunities. *Remote Sensing of Environment*, 232, 111291. <https://doi.org/10.1016/j.rse.2019.111291>
- Wilhite, D. A., & Glantz, M. H. (1985). Understanding: The drought phenomenon: The role of definitions. *Water International*, 10(3), 111–120. <https://doi.org/10.1080/02508068508686328>
- Wilks, D. S., & Eggleston, K. L. (1992). Estimating monthly and seasonal precipitation distributions using the 30-and 90-day outlooks. *Journal of Climate*, 5(3), 252–259. [https://doi.org/10.1175/1520-0442\(1992\)005<0252:emaspd>2.0.co;2](https://doi.org/10.1175/1520-0442(1992)005<0252:emaspd>2.0.co;2)
- Wu, J., Chen, X., Gao, L., Yao, H., Chen, Y., & Liu, M. (2016). Response of hydrological drought to meteorological drought under the influence of large reservoir. *Advances in Meteorology*, 2016, 1–11. <https://doi.org/10.1155/2016/2197142>
- Wu, J., Chen, X., Yao, H., Gao, L., Chen, Y., & Liu, M. (2017). Non-linear relationship of hydrological drought responding to meteorological drought and impact of a large reservoir. *Journal of Hydrology*, 551, 495–507. <https://doi.org/10.1016/j.jhydrol.2017.06.029>
- Wu, J., Miao, C., Zheng, H., Duan, Q., Lei, X., & Li, H. (2018). Meteorological and hydrological drought on the Loess Plateau, China: Evolutionary characteristics, impact, and propagation. *Journal of Geophysical Research: Atmospheres*, 123(20), 11569–11584. <https://doi.org/10.1029/2018jd029145>
- Wu, J., Wang, Z., Li, W., & Peng, J. (2013). Exploring factors affecting the relationship between light consumption and GDP based on DMSP/OLS nighttime satellite imagery. *Remote Sensing of Environment*, 134, 111–119. <https://doi.org/10.1016/j.rse.2013.03.001>
- Wu, J., Yao, H., Chen, X., Wang, G., Bai, X., & Zhang, D. (2022). A framework for assessing compound drought events from a drought propagation perspective. *Journal of Hydrology*, 604, 127228. <https://doi.org/10.1016/j.jhydrol.2021.127228>
- Wu, J., Zhou, L., Mo, X., Zhou, H., Zhang, J., & Jia, R. (2015). Drought monitoring and analysis in China based on the integrated surface drought index (ISDI). *International Journal of Applied Earth Observation and Geoinformation*, 41, 23–33. <https://doi.org/10.1016/j.jag.2015.04.006>
- Wu, Z., Mao, Y., Li, X., Lu, G., Lin, Q., & Xu, H. (2015). Exploring spatiotemporal relationships among meteorological, agricultural, and hydrological droughts in Southwest China. *Stochastic Environmental Research and Risk Assessment*, 30(3), 1033–1044. <https://doi.org/10.1007/s00477-015-1080-y>
- Xing, Z., Ma, M., Zhang, X., Leng, G., Su, Z., Lv, J., et al. (2021). Altered drought propagation under the influence of reservoir regulation. *Journal of Hydrology*, 603, 127049. <https://doi.org/10.1016/j.jhydrol.2021.127049>
- Xu, Y., Zhang, X., Hao, Z., Singh, V. P., & Hao, F. (2021). Characterization of agricultural drought propagation over China based on bivariate probabilistic quantification. *Journal of Hydrology*, 598, 126194. <https://doi.org/10.1016/j.jhydrol.2021.126194>
- Xu, Y., Zhang, X., Wang, X., Hao, Z., Singh, V. P., & Hao, F. (2019). Propagation from meteorological drought to hydrological drought under the impact of human activities: A case study in northern China. *Journal of Hydrology*, 579, 124147. <https://doi.org/10.1016/j.jhydrol.2019.124147>
- Xu, Y., Zhu, X., Cheng, X., Gun, Z., Lin, J., Zhao, J., et al. (2022). Drought assessment of China in 2002–2017 based on a comprehensive drought index. *Agricultural and Forest Meteorology*, 319, 108922. <https://doi.org/10.1016/j.agrformet.2022.108922>
- Yang, F., Duan, X., Guo, Q., Lu, S., & Hsu, K. (2021). The spatiotemporal variations and propagation of droughts in Plateau Mountains of China. *Science of the Total Environment*, 805, 150257. <https://doi.org/10.1016/j.scitotenv.2021.150257>
- Yang, X., Zhang, M., He, X., Ren, L., Pan, M., Yu, X., et al. (2020). Contrasting influences of human activities on hydrological drought regimes over China based on high-resolution simulations. *Water Resources Research*, 56(6), e2019WR025843. <https://doi.org/10.1029/2019wr025843>
- Yao, N., Li, Y., Li, N., Yang, D., & Ayantobo, O. O. (2018). Bias correction of precipitation data and its effects on aridity and drought assessment in China over 1961–2015. *Science of the Total Environment*, 639, 1015–1027. <https://doi.org/10.1016/j.scitotenv.2018.05.243>

- Yevjevich, V. M. (1967). *An objective approach to definitions and investigations of continental hydrologic droughts*. Colorado State University.
- Zhang, A., & Jia, G. (2013). Monitoring meteorological drought in semiarid regions using multi-sensor microwave remote sensing data. *Remote Sensing of Environment*, *134*, 12–23. <https://doi.org/10.1016/j.rse.2013.02.023>
- Zhang, H., Ding, J., Wang, Y., Zhou, D., & Zhu, Q. (2021). Investigation about the correlation and propagation among meteorological, agricultural and groundwater droughts over humid and arid/semi-arid basins in China. *Journal of Hydrology*, *603*, 127007. <https://doi.org/10.1016/j.jhydrol.2021.127007>
- Zhang, Q., Miao, C., Gou, J., Wu, J., Jiao, W., Song, Y., & Xu, D. (2022). Spatiotemporal characteristics of meteorological to hydrological drought propagation under natural conditions in China. *Weather and Climate Extremes*, *38*, 200505. <https://doi.org/10.1016/j.wace.2022.100505>
- Zhang, Q., & Seto, K. C. (2011). Mapping urbanization dynamics at regional and global scales using multi-temporal DMSP/OLS nighttime light data. *Remote Sensing of Environment*, *115*(9), 2320–2329. <https://doi.org/10.1016/j.rse.2011.04.032>
- Zhang, R., Sumi, A., & Kimoto, M. (1999). A diagnostic study of the impact of El Niño on the precipitation in China. *Advances in Atmospheric Sciences*, *16*(2), 229–241. <https://doi.org/10.1007/bf02973084>
- Zhang, T., Su, X., Zhang, G., Wu, H., Wang, G., & Chu, J. (2022). Evaluation of the impacts of human activities on propagation from meteorological drought to hydrological drought in the Weihe River Basin, China. *Science of the Total Environment*, *819*, 153030. <https://doi.org/10.1016/j.scitotenv.2022.153030>
- Zhang, X., Chen, N., Li, J., Chen, Z., & Niyogi, D. (2017). Multi-sensor integrated framework and index for agricultural drought monitoring. *Remote Sensing of Environment*, *188*, 141–163. <https://doi.org/10.1016/j.rse.2016.10.045>
- Zhang, Y., Hao, Z., Feng, S., Zhang, X., Xu, Y., & Hao, F. (2021). Agricultural drought prediction in China based on drought propagation and large-scale drivers. *Agricultural Water Management*, *255*, 107028. <https://doi.org/10.1016/j.agwat.2021.107028>
- Zhao, B., Yang, D., Yang, S., & Santisirisomboon, J. (2022). Spatiotemporal characteristics of droughts and their propagation during the past 67 Years in northern Thailand. *Atmosphere*, *13*(2), 277. <https://doi.org/10.3390/atmos13020277>
- Zhong, R., Chen, X., Lai, C., Wang, Z., Lian, Y., Yu, H., & Wu, X. (2019). Drought monitoring utility of satellite-based precipitation products across mainland China. *Journal of Hydrology*, *568*, 343–359. <https://doi.org/10.1016/j.jhydrol.2018.10.072>
- Zhou, K., Li, J., Zhang, T., & Kang, A. (2021). The use of combined soil moisture data to characterize agricultural drought conditions and the relationship among different drought types in China. *Agricultural Water Management*, *243*, 106479. <https://doi.org/10.1016/j.agwat.2020.106479>
- Zhou, Z., Shi, H., Fu, Q., Ding, Y., Li, T., & Liu, S. (2021a). Investigating the propagation from meteorological to hydrological drought by introducing the nonlinear dependence with directed information transfer index. *Water Resources Research*, *57*(8), e2021WR030028. <https://doi.org/10.1029/2021wr030028>
- Zhou, Z., Shi, H., Fu, Q., Ding, Y., Li, T., Wang, Y., & Liu, S. (2021b). Characteristics of propagation from meteorological drought to hydrological drought in the Pearl River Basin. *Journal of Geophysical Research: Atmospheres*, *126*(4), e2020JD033959. <https://doi.org/10.1029/2020jd033959>
- Zhu, Y., Liu, Y., Wang, W., Singh, V. P., & Ren, L. (2021). A global perspective on the probability of propagation of drought: From meteorological to soil moisture. *Journal of Hydrology*, *603*, 126907. <https://doi.org/10.1016/j.jhydrol.2021.126907>
- Zhu, Y., Wang, W., Singh, V. P., & Liu, Y. (2016). Combined use of meteorological drought indices at multi-time scales for improving hydrological drought detection. *Science of the Total Environment*, *571*, 1058–1068. <https://doi.org/10.1016/j.scitotenv.2016.07.096>

References From the Supporting Information

- Gullacher, A., Allen, D., & Goetz, J. (2023). Early warning indicators of groundwater drought in mountainous regions. *Water Resources Research*, *59*(8), e2022WR033399. <https://doi.org/10.1029/2022wr033399>
- Han, J., Wang, J., Chen, L., Xiang, J., Ling, Z., Li, Q., & Wang, E. (2021). Driving factors of desertification in Qaidam Basin, China: An 18-year analysis using the geographic detector model. *Ecological Indicators*, *124*, 107404. <https://doi.org/10.1016/j.ecolind.2021.107404>
- Han, Z., Huang, S., Zhao, J., Leng, G., Huang, Q., Zhang, H., & Li, Z. (2023). Long-chain propagation pathways from meteorological to hydrological, agricultural and groundwater drought and their dynamics in China. *Journal of Hydrology*, *625*, 130131. <https://doi.org/10.1016/j.jhydrol.2023.130131>
- Li, W., Reichstein, M., O, S., May, C., Destouni, G., Migliavacca, M., et al. (2023). Contrasting drought propagation into the terrestrial water cycle between dry and wet regions. *Earth's Future*, *11*(7), e2022EF003441. <https://doi.org/10.1029/2022ef003441>
- Qiao, P., Yang, S., Lei, M., Chen, T., & Dong, N. (2019). Quantitative analysis of the factors influencing spatial distribution of soil heavy metals based on geographical detector. *Science of the Total Environment*, *664*, 392–413. <https://doi.org/10.1016/j.scitotenv.2019.01.310>
- Van Lanen, H. A., Wanders, N., Tallaksen, L. M., & Van Loon, A. F. (2013). Hydrological drought across the world: Impact of climate and physical catchment structure. *Hydrology and Earth System Sciences*, *17*(5), 1715–1732. <https://doi.org/10.5194/hess-17-1715-2013>
- Wood, S. N. (2004). Stable and efficient multiple smoothing parameter estimation for generalized additive models. *Journal of the American Statistical Association*, *99*(467), 673–686. <https://doi.org/10.1198/016214504000000980>
- Wood, S. N. (2017). *Generalized additive models: An introduction with R* [Software]. CRC Press. <https://doi.org/10.1201/9781315370279>
- Wood, S. N., Goude, Y., & Shaw, S. (2015). Generalized additive models for large data sets. *Journal of the Royal Statistical Society Series C: Applied Statistics*, *64*(1), 139–155. <https://doi.org/10.1111/rssc.12068>